Pergamon

Int. J. Solids Structures Vol. 32, No. 2, pp. 137–163, 1995

0020-7683/95 $9.50 + .00

0020-7683(94)00140-5

DERIVATION OF THE IN-PLANE ELASTIC CHARACTERISTICS OF MASONRY THROUGH HOMOGENIZATION THEORY

A. ANTHOINE
Applied Mechanics Unit, Institute for Safety Technology, Joint Research Centre, European Commission I-21020 Ispra (VA), Italy

(*Received* 12 *November* 1993; *in revised form* 12 *June* 1994)

Abstract—The homogenization theory for periodic media allows the global behaviour of masonry to be derived from the behaviour of the constitutive materials (brick and mortar). Such a procedure has been used by many authors but always in an approximate manner. In particular, the homogenization procedure has always been performed in several successive steps, head joints and bed joints being introduced successively. Moreover, masonry was considered either as a two-dimensional media under the plane stress assumption (very thin media), or as a three-dimensional bulk (very thick media), so that its finite thickness was never taken into account.

The homogenization theory for periodic media is implemented here in a rigorous way, i.e. in one step and on the real geometry of masonry (finite thickness and actual bond pattern). Numerical applications are carried out and the results are compared with the predictions based on existing simplified approaches. All the above-mentioned approximations turn out to slightly affect the in-plane elastic characteristics of masonry, but it is anticipated that, in the non-linear range (plasticity or damage), the same approximations might lead to erroneous results, quantitatively as well as qualitatively (value of the ultimate load and mode of failure).

1. INTRODUCTION

Masonry may be considered as a periodic composite continuum; it is made up of two different materials (brick and mortar) arranged in a periodic way. The homogenization theory for periodic media allows the global behaviour of masonry to be derived from the behaviour of the constitutive materials. This procedure has been used by many authors such as Maier *et al.* (1991), Pande *et al.* (1989) or Pietruszczak and Niu (1992), but only in an approximate manner.

- The homogenization procedure has always been performed in several steps, head joints and bed joints being introduced successively. Such a methodology introduces two sources of error: first, the result generally depends on the order of the successive steps, as shown by Geymonat *et al.* (1987); second, the geometrical arrangement is not fully taken into account in the sense that different bond patterns (running bond and stack bond for example) may lead to exactly the same result.
- The homogenization procedure itself was sometimes approximate [self consistent method in Pietruszczak and Niu (1992)].
- The geometry of the arrangement was often simplified, mortar joints being treated as interfaces or ellipsoidal inclusions [Pietruszczak and Niu (1992)].
- Finally, the thickness of masonry was never taken into account because masonry was considered either as infinitely thin [two-dimensional media under the plane stress assumption in Maier *et al.* (1991) and Pande *et al.* (1989)], or as infinitely thick [three-dimensional bulk in Pande *et al.* (1989) and Pietruszczak and Niu (1992)].

The aim of this paper is to derive the in-plane elastic characteristics of masonry through a rigorous application of the homogenization theory for periodic media, that is in one step, on the exact geometry and taking into account the finite thickness of masonry. First, the main results of the homogenization theory for periodic media are retrieved heuristically, in the case of two-dimensional media. Such an intuitive reasoning is then easily extended to

the case of three-dimensional media having only two directions of periodicity and a finite thickness, such as masonry walls. Finally, numerical applications are carried out in linear elasticity and the results are compared with the predictions based on other simplified formulations: special attention is then given to the influence of the bond pattern (running bond versus stack bond) of the thickness (plane stress assumption, bulk assumption, finite thickness), and of the order of the successive steps (head joints first versus bed joints first).

2. HEURISTIC PRESENTATION OF THE HOMOGENIZATION THEORY FOR TWO-DIMENSIONAL PERIODIC MEDIA

The principles of the homogenization theory are presented here in a rather intuitive way, using only basic mechanics and mathematics. This presentation is mainly directed to people who are not yet familiar with this theory. Most technical aspects such as functional settings, existence and uniqueness theorems, convergence properties, etc. are deliberately avoided. Complete and technical presentations based on asymptotic analysis may be found in the literature (Bensoussan *et al.*, 1978; Duvaut, 1984; Sanchez-Palencia, 1980).

For the sake of simplicity, only two-dimensional periodic media are considered in this first part, i.e. three-dimensional media under the plane stress or plane strain assumption, for example. Since it is intended to apply the homogenization theory to masonry, typical "masonry like" patterns are considered; rectangles (bricks) arranged in stack bond or running bond with regular head and bed joints (mortar). However, the presentation remains valid for any type of two-dimensional periodic media (perforated sheet under plane stress or fibre reinforced composites under plane strain for instance).

2.1. *Description of a two-dimensional periodic composite media*

Consider a portion of masonry wall under the plane stress assumption (Fig. 1). It is a two-dimensional periodic composite continuum, made up of two different materials (brick and mortar) arranged in a periodic way (running bond). The periodicity may be characterized by a frame of reference $(\mathbf{v}_1, \mathbf{v}_2)$, where $\mathbf{v}_1$ and $\mathbf{v}_2$ are two independent vectors having the following property: the mechanical characteristics of the media are invariant along any translation $m_1\mathbf{v}_1 + m_2\mathbf{v}_2$, where m_1 and m_2 are integers (Fig. 1). As a consequence, it is enough to define the mechanical properties of the media on a small domain S (cell) to be repeated by translation. The most natural choice of cell is the parallelogram spanned by the vectors of the frame of reference (Fig. 2, left). Neither the frame of reference, nor the associated cell is uniquely defined. However, for a given frame of reference $(\mathbf{v}_1, \mathbf{v}_2)$, all possible cells have the same area $|S|$ which is equal to the norm of the vector product $|\mathbf{v}_1 \wedge \mathbf{v}_2|$ (Fig. 2, right). Furthermore, the boundary ∂S of a cell S can always be divided into two or three pairs of identical sides corresponding to each other through a translation along $\mathbf{v}_1, \mathbf{v}_2$ or $\mathbf{v}_1 - \mathbf{v}_2$ (Fig. 2). Two such sides will be said to be opposite. Since finite element calculations are to be performed on the cell, it is worth choosing it with the least area and, if possible, with symmetry properties. Such minimum cells and associated frames of reference will be called basic. The choice of the basic cell depends strongly on the geometry of the composite media. In the case of common masonry patterns (stack bond or running bond), a "good"

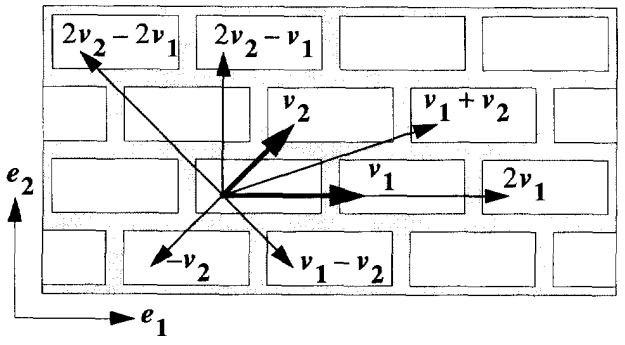

Fig. 1. Two-dimensional running bond masonry (plane stress) and frame of reference.

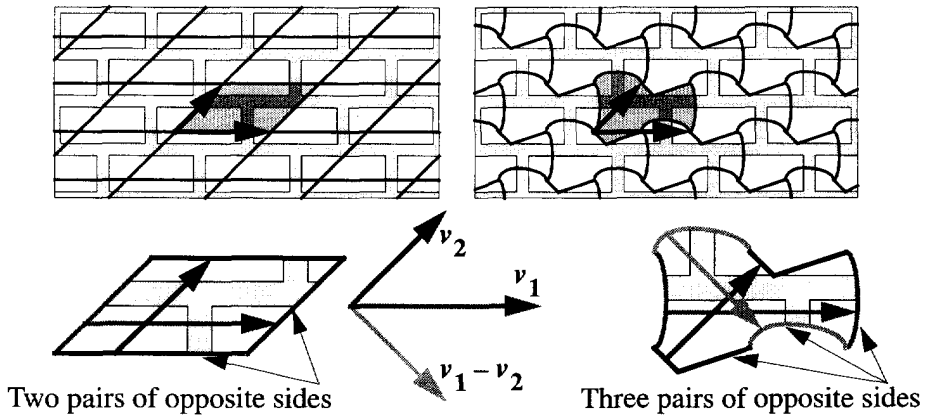

Fig. 2. Two different cells associated to the same frame of reference and having, respectively, two and three pairs of opposite sides.

basic cell is made up of one brick surrounded by half mortar joint. The reference frame is then composed of

$$\begin{aligned} \mathbf{v}_1 &= 2l\mathbf{e}_1 \\ \mathbf{v}_2 &= d\mathbf{e}_1 + 2h\mathbf{e}_2, \end{aligned} \tag{1}$$

where $2l$ is equal to the length of the brick plus the thickness of the head joint, $2h$ is equal to the height of the brick plus the thickness of the bed joint and d is the overlapping (Fig. 3): $d = 0$ gives stack bond, $d = l$ gives running bond and $d = (2/3)l$ gives a bond which should not be confused with 1/3 running bond (Fig. 4). Note that the same basic cell S leads to different patterns when associated to different frames of reference. The boundary ∂S of the cell is composed of three pairs of opposite sides (vertical sides, upper left with lower right, upper right with lower left) which reduce to two pairs (parallel sides of the rectangle) in the case of the stack bond pattern. More complex bonds would require greater cells, i.e. cells involving more than one brick. In the literature, distinction is often made between rectangular patterns and hexagonal patterns. As a matter of fact, the formers are particular cases of the latters; rectangular patterns admit an orthogonal basic frame whereas hexagonal ones do not. Nevertheless, both admit a rectangular basic cell. Stack bond, 1/3 running bond and English bond are rectangular patterns; running bond, Flemish bond and Dutch bond are hexagonal patterns (Fig. 4).

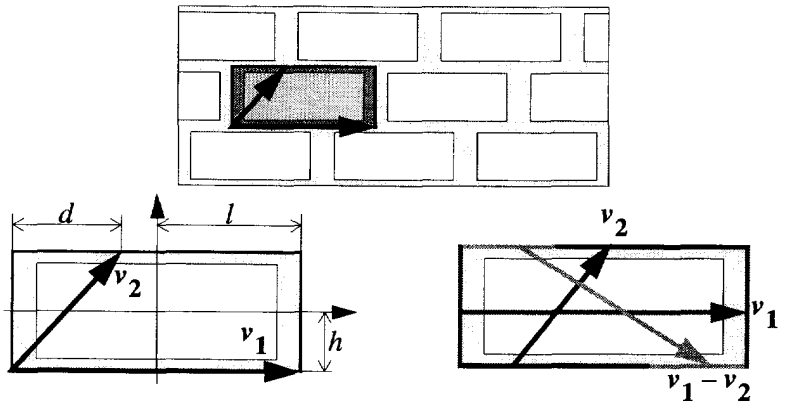

Fig. 3. Frame of reference, basic cell and opposite sides for common masonry patterns: $d = 0$ for stack bond; $d = l$ for running bond.

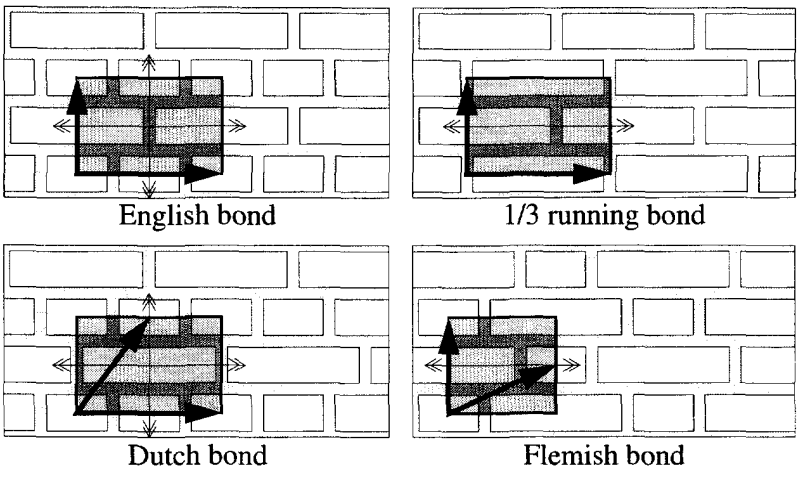

Fig. 4. Basic cell and frame of reference for more complex bond patterns.

2.2. *Periodic stresses, strain–periodic displacements*

Suppose now that a portion Ω of masonry is subjected to a globally homogeneous stress state. A stress state is said to be globally or macroscopically homogeneous over a domain Ω if all cells within Ω undergo the same loading conditions. This can be approximately achieved with an experimental set-up designed to apply any biaxial principal stress state to a panel (Dhanasekar *et al.*, 1982). The shear stress component is then obtained by selecting the proper lay-up angle of the specimen (Fig. 5). The approximation is due to perturbations near the boundary; a cell lying near the boundary $\partial\Omega$ of the specimen is not subjected to the same loading as one lying in the centre. However, on account of the Saint-Venant principle, cells lying far enough from the boundary are subjected to the same loading conditions and therefore deform in the same way. In particular, two joined cells must still fit together in their common deformed state, just like in a picture of Escher (Fig. 6). In mechanical terms, this means that, when passing from a cell to the next one, (i) the stress vector $\boldsymbol{\sigma}\cdot\mathbf{n}$ is continuous; (ii) strains are compatible, i.e. neither separation nor overlapping occurs. Since passing from a cell to the next one which is identical, also means passing from a side to the opposite one in the same cell S, condition (i) becomes

$$\text{stress vectors } \boldsymbol{\sigma}\cdot\mathbf{n} \text{ are opposite on opposite sides of } \partial S \tag{2}$$

because external normal $\mathbf{n}$ are also opposite. Such a stress field $\boldsymbol{\sigma}$ is said to be periodic on

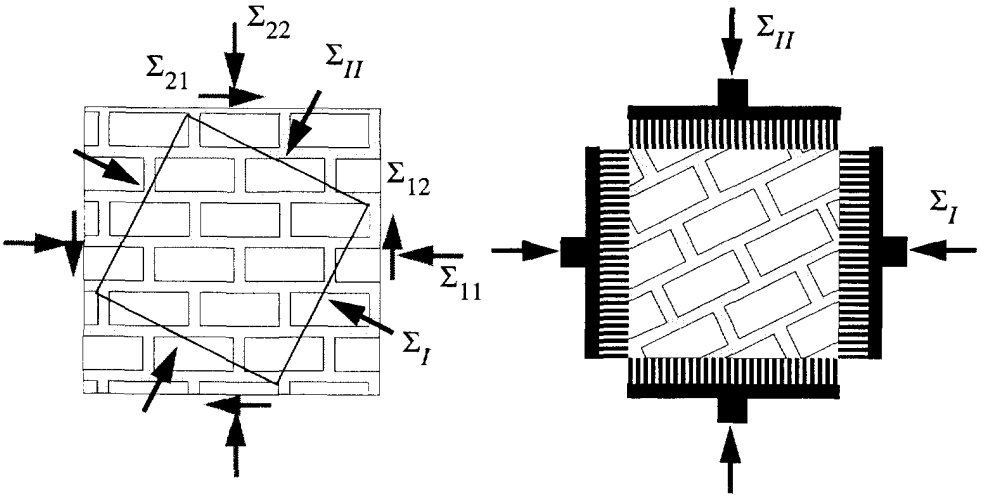

Fig. 5. Macroscopically homogeneous stress state test [testing set-up from Dhanasekar *et al.* (1982)].

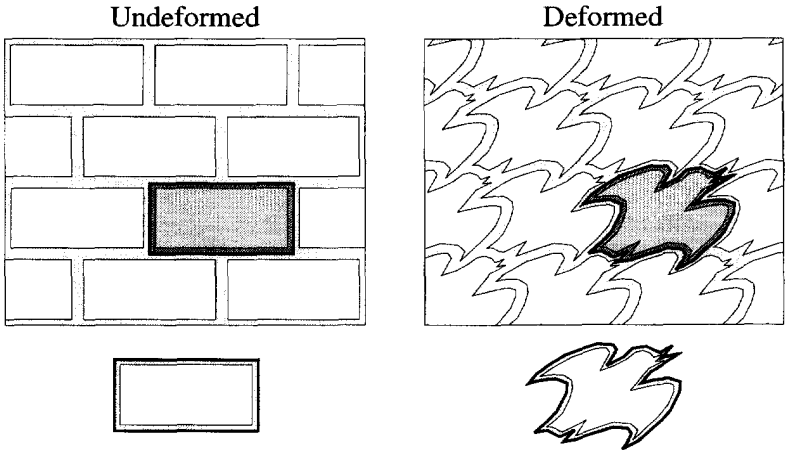

Fig. 6. Escher-like picture illustrating the concept of macroscopic homogeneity.

∂S, whereas the external normal $\mathbf{n}$ and the stress vector $\boldsymbol{\sigma}\cdot\mathbf{n}$ are said to be anti-periodic on ∂S.

To ensure condition (ii), it is necessary that opposite sides can be superimposed in their deformed states. In other words, the displacement fields on two opposite sides must be equal up to a rigid displacement. In the case of stack bond pattern (Fig. 7, left), this is expressed by

$$\begin{aligned} &\forall x_2 \in [-h, h], \mathbf{u}(l, x_2) - \mathbf{u}(-l, x_2) = \mathbf{U} - Rx_2\mathbf{e}_1 \\ &\forall x_1 \in [-l, l], \mathbf{u}(x_1, h) - \mathbf{u}(x_1, -h) = \mathbf{V} + Sx_1\mathbf{e}_2, \end{aligned} \tag{3}$$

where $\mathbf{U}$ and $\mathbf{V}$ are translation vectors and R and S are rotation constants. Of course, each corner of the cell must undergo the same displacement when considered to belong either to a vertical or a horizontal side. This means that relations (3) must be compatible when written for extreme values of x_1 and x_2:

$$\begin{aligned} x_2 &= h \Rightarrow \mathbf{u}(l, h) - \mathbf{u}(-l, h) = \mathbf{U} - Rh\mathbf{e}_1 \\ x_2 &= -h \Rightarrow \mathbf{u}(l, -h) - \mathbf{u}(-l, -h) = \mathbf{U} + Rh\mathbf{e}_1 \\ x_1 &= l \Rightarrow \mathbf{u}(l, h) - \mathbf{u}(l, -h) = \mathbf{V} + Sl\mathbf{e}_2 \\ x_1 &= -l \Rightarrow \mathbf{u}(-l, h) - \mathbf{u}(-l, -h) = \mathbf{V} - Sl\mathbf{e}_2. \end{aligned} \tag{4}$$

This is ensured only if R and S are zero constants. A very similar result may be proved in the case of running bond pattern, provided that a parallelogram cell is considered (Fig. 7, right). System (3) then changes to

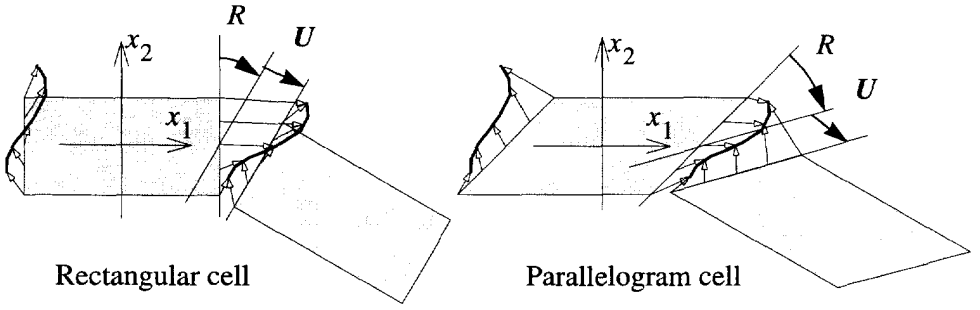

Fig. 7. Strain compatibility through one side of a rectangular (left) or parallelogram (right) basic cell.

$$\forall x_2 \in [-h,h], \mathbf{u}\left(l+\frac{lx_2}{2h}, x_2\right)-\mathbf{u}\left(-l+\frac{lx_2}{2h}, x_2\right) = \mathbf{U}-R\left(x_2\mathbf{e}_1+\frac{lx_2}{2h}\mathbf{e}_2\right)$$

$$\forall x_1 \in [-l,l], \mathbf{u}\left(\frac{l}{2}+x_1, h\right)-\mathbf{u}\left(-\frac{l}{2}+x_1, -h\right) = \mathbf{V}+Sx_1\mathbf{e}_2. \tag{5}$$

Again, displacements at corners are consistent only if R and S are zero constants. System (3) and (5) both reduce to

$$\forall x_2 \in [-h,h], \mathbf{u}\left(l+\frac{dx_2}{2h}, x_2\right)-\mathbf{u}\left(-l+\frac{dx_2}{2h}, x_2\right) = \mathbf{U}$$

$$\forall x_1 \in [-l,l], \mathbf{u}\left(\frac{d}{2}+x_1, h\right)-\mathbf{u}\left(-\frac{d}{2}+x_1, -h\right) = \mathbf{V}, \tag{6}$$

where d still stands for the overlapping. Since it leads to a periodic strain field, such a displacement field $\mathbf{u}$ is called strain–periodic. It is easy to show that a strain–periodic displacement field $\mathbf{u}$ may always be written in the following form:

$$\forall \alpha, \beta = 1 \text{ or } 2, u_\alpha(x_1,x_2) = E_{\alpha\beta}x_\beta + u^{\mathrm{p}}_\alpha(x_1,x_2) \Leftrightarrow \mathbf{u}(x_1,x_2) = \mathbf{E}\cdot\mathbf{x}+\mathbf{u}^{\mathrm{p}}(x_1,x_2), \tag{7}$$

where $E_{\alpha\beta}$ are constants and $\mathbf{u}^{\mathrm{p}}$ is a periodic displacement field; $\mathbf{u}^{\mathrm{p}}$ takes equal values on opposite sides of ∂S. The equivalence between (6) and (7) is obtained by taking

$$\begin{aligned} E_{11} &= U_1/2l \\ E_{21} &= U_2/2l \\ E_{12} &= (V_1 - U_1 d/2l)/2h \\ E_{22} &= (V_2 - U_2 d/2l)/2h. \end{aligned} \tag{8}$$

Relations (8) show that E_{11} represents the mean elongation of the cell along the first axis and, more generally, that $\mathbf{E}$ is the mean strain tensor of the cell. In particular, the anti-symmetric part of $\mathbf{E}$ corresponds indeed to a rigid rotation of the cell. As a consequence, only the symmetric part of $\mathbf{E}$ may be considered (rigid displacements are disregarded). This interpretation of $\mathbf{E}$ is consistent with the intuitive definition of the average $\langle Q \rangle$ of a quantity Q on the cell

$$\langle Q \rangle = \frac{\int_S Q \,\mathrm{d}s}{\int_S \mathrm{d}s} = \frac{1}{|S|}\int_S Q \,\mathrm{d}s, \tag{9}$$

where $|S|$ stands for the area of the cell S ($|S| = |\mathbf{v}_1 \wedge \mathbf{v}_2|$). If Q is a vectorial or tensorial quantity, definition (9) holds for each component of Q. Thus, if Q stands for $\varepsilon_{\alpha\beta}(\mathbf{u})$,

$$\langle \varepsilon_{\alpha\beta}(\mathbf{u}) \rangle = \frac{1}{|S|}\int_S \varepsilon_{\alpha\beta}(\mathbf{u}) \,\mathrm{d}s. \tag{10}$$

From (7) and the definition of $\varepsilon_{\alpha\beta}(\mathbf{u})$ as the symmetric part of the gradient of $\mathbf{u}$, it follows that

$$\varepsilon_{\alpha\beta}(\mathbf{u}) = (E_{\alpha\beta} + u^{\mathrm{p}}_{\alpha,\beta} + E_{\beta\alpha} + u^{\mathrm{p}}_{\beta,\alpha})/2 = E_{\alpha\beta} + (u^{\mathrm{p}}_{\alpha,\beta} + u^{\mathrm{p}}_{\beta,\alpha})/2 \tag{11}$$

since $\mathbf{E}$ has been assumed symmetric. By introducing (11) into (10), one gets

$$\langle \varepsilon_{\alpha\beta}(\mathbf{u}) \rangle = E_{\alpha\beta} + \frac{1}{2|S|} \int_S (u^{\mathrm{p}}_{\alpha,\beta} + u^{\mathrm{p}}_{\beta,\alpha})\, \mathrm{d}s. \tag{12}$$

By integrating by parts, using the divergence theorem, it follows that

$$\langle \varepsilon_{\alpha\beta}(\mathbf{u}) \rangle = E_{\alpha\beta} + \frac{1}{2|S|} \int_{\partial S} (u^{\mathrm{p}}_{\alpha} n_{\beta} + u^{\mathrm{p}}_{\beta} n_{\alpha})\, \mathrm{d}l. \tag{13}$$

Since $\mathbf{u}^{\mathrm{p}}$ and $\mathbf{n}$ are respectively periodic and anti-periodic vector fields on ∂S, $u^{\mathrm{p}}_{\alpha} n_{\beta}$ is an anti-periodic scalar field on ∂S and, thus, its integral on ∂S vanishes (values on opposite sides cancel each other). Therefore, $\mathbf{E}$ turns out to coincide with the average of $\boldsymbol{\varepsilon}(\mathbf{u})$ on the cell

$$\langle \varepsilon_{\alpha\beta}(\mathbf{u}) \rangle = E_{\alpha\beta} \Leftrightarrow \langle \boldsymbol{\varepsilon}(\mathbf{u}) \rangle = \mathbf{E}. \tag{14}$$

By introducing (14) into (7), the following definition is derived:

$$\mathbf{u} \text{ strain–periodic} \Leftrightarrow \mathbf{u} - \langle \boldsymbol{\varepsilon}(\mathbf{u}) \rangle \cdot \mathbf{x} \text{ periodic}. \tag{15}$$

By analogy with (10), it is natural to introduce the average of $\sigma_{\alpha\beta}$ on the cell by

$$\langle \sigma_{\alpha\beta} \rangle = \frac{1}{|S|} \int_S \sigma_{\alpha\beta}\, \mathrm{d}s. \tag{16}$$

By definition, $\langle \sigma_{\alpha\beta} \rangle$ is the so-called macroscopic stress component and will be noted $\Sigma_{\alpha\beta}$. This is coherent with the fact that, in the case of the specimen shown on Fig. 5, $\boldsymbol{\Sigma}$ coincides with the stress applied to the specimen (this may be shown provided that the perturbations near the boundary are disregarded).

If the basic cell includes a cavity Γ, definitions (10) and (16) need to be clarified since $\boldsymbol{\sigma}$ and $\boldsymbol{\varepsilon}(\mathbf{u})$ are not defined within Γ. However, considering voids as infinitely soft inclusions on which $\boldsymbol{\sigma}$ vanishes, definition (16) becomes

$$\langle \boldsymbol{\sigma} \rangle = \frac{1}{|S|} \int_{S^*} \boldsymbol{\sigma}\, \mathrm{d}s, \tag{17}$$

where S^* is the material part of S ($S^* = S - \Gamma$) and $|S|$ is still the total area of S ($|S| = |\mathbf{v}_1 \wedge \mathbf{v}_2|$). As far as strains are concerned, definition (10) may be transformed into a boundary integral through the divergence theorem

$$\langle \varepsilon_{\alpha\beta}(\mathbf{u}) \rangle = \frac{1}{2|S|} \int_{\partial S} (u_{\alpha} n_{\beta} + u_{\beta} n_{\alpha})\, \mathrm{d}l. \tag{18}$$

Such a definition turns out to remain valid in the case of a perforated cell provided that the

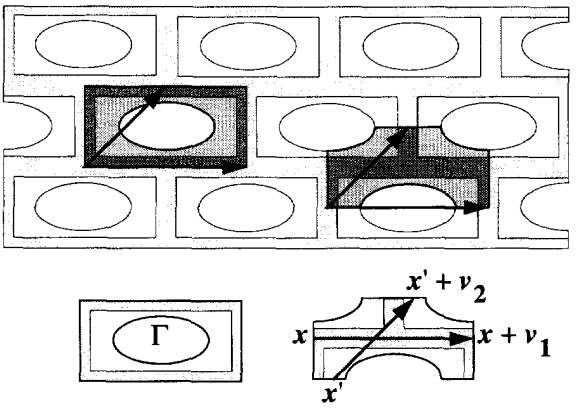

Fig. 8. Basic cells including cavities intersecting the boundary (right) or not (left).

holes do not intersect the boundary ∂S (Fig. 8, left); in dimension two, such a choice is always possible. Re-transforming (18) through the divergence theorem, one gets

$$\langle \varepsilon_{\alpha\beta}(\mathbf{u}) \rangle = \frac{1}{|S|} \int_{S^*} \varepsilon_{\alpha\beta}(\mathbf{u}) \, \mathrm{d}s - \frac{1}{2|S|} \int_{\partial\Gamma} (u_\alpha n_\beta + u_\beta n_\alpha) \, \mathrm{d}l, \tag{19}$$

where $\partial\Gamma$ is the boundary of the cavity ($\mathbf{n}$ points inside Γ). Expression (19) shows that the deformation of the cell is composed of two terms: the deformation of the material part S^* (first integral) and the shape change of the hole (second integral).

Expressions (17) and (18) [or (19)] are of practical interest since their use in a finite element code does not require the discretization of the holes. However, unlike expression (17), expressions (18) and (19) are restricted to a particular choice of the basic cell (the eventual holes should not intersect the boundary). A way to get rid of this last restriction is to use the original definition of the average strain $\mathbf{E}$. According to expression (7), if $\mathbf{x}$ and $(\mathbf{x}+\mathbf{t})$ are two opposite points of ∂S (i.e. if $\mathbf{t}$ is equal to $\mathbf{v}_1$, $\mathbf{v}_2$ or $\mathbf{v}_1 - \mathbf{v}_2$), their corresponding displacements verify

$$u_\alpha^{\mathrm{P}}(\mathbf{x}+\mathbf{t}) = u_\alpha^{\mathrm{P}}(\mathbf{x}) \Rightarrow u_\alpha(\mathbf{x}+\mathbf{t}) - u_\alpha(\mathbf{x}) = E_{\alpha\beta} t_\beta. \tag{20}$$

Writing relation (14) for another pair of opposite points related by a vector $\mathbf{t}'$ linearly independent of $\mathbf{t}$, one gets a linear system giving $\mathbf{E}$ and thus the symmetric part of $\mathbf{E}$, in terms of $\mathbf{v}_1$, $\mathbf{v}_2$ and of the displacements $\mathbf{u}$ at four particular points of the boundary of the cell. It is always possible to choose those four points in the material part of the cell, even if holes intersect the boundary (Fig. 8, right). Note that this last definition of the average strain has a sense (i.e. is independent of the choice of the four points) only for strain–periodic displacement fields, whereas definitions (18) or (19) may be applied to any displacement fields, whether strain–periodic or not.

2.3. *Homogenization*

Let us still consider the problem of a masonry specimen subjected to a macroscopically homogeneous stress state $\mathbf{\Sigma}$. The previous section was devoted to the special conditions holding on the boundary ∂S of any cell S; $\boldsymbol{\sigma}$ is periodic and $\mathbf{u}$ is strain–periodic. Those conditions make it possible to study the problem within a single cell rather than on the whole specimen. In order to find $\boldsymbol{\sigma}$ and $\mathbf{u}$ everywhere in a cell, equilibrium conditions and constitutive relationships must be added so that the problem to solve is

$$\operatorname{div} \boldsymbol{\sigma} = \mathbf{0} \text{ on } S \text{ (no body forces)}$$

$$\boldsymbol{\sigma} = f(\boldsymbol{\varepsilon}(\mathbf{u})) \text{ (constitutive law under plane stresses)}$$

$$\begin{aligned} &\boldsymbol{\sigma} \text{ periodic on } \partial S \,(\boldsymbol{\sigma}\cdot\mathbf{n} \text{ anti-periodic on } \partial S)\\ &\mathbf{u} - \langle \boldsymbol{\varepsilon}(\mathbf{u})\rangle \cdot \mathbf{x} \,(\text{periodic on } \partial S)\\ &\langle \boldsymbol{\sigma}\rangle = \boldsymbol{\Sigma},\ \boldsymbol{\Sigma} \text{ given (stress controlled loading),} \end{aligned} \tag{21}$$

where the constitutive law f is a periodic function of the spatial variable $\mathbf{x}$ since it describes the behaviour of the different materials in the composite cell.

A problem similar to (21) is obtained when replacing the stress controlled loading by a strain controlled one:

$$\langle \boldsymbol{\varepsilon}(\mathbf{u})\rangle = \mathbf{E},\ \mathbf{E} \text{ given.} \tag{21a}$$

In both cases, the resolution of (21) is sometimes termed "localization" because the local (microscopic) fields $\boldsymbol{\sigma}$ and $\boldsymbol{\varepsilon}(\mathbf{u})$ are determined from the global (macroscopic) quantity $\boldsymbol{\Sigma}$ or $\mathbf{E}$.

It is worth noting that, independently of the constitutive laws of the materials, the average procedure holds true in an energetic sense, i.e.

$$\langle \boldsymbol{\sigma} : \boldsymbol{\varepsilon}(\mathbf{u})\rangle = \langle \boldsymbol{\sigma}\rangle : \langle \boldsymbol{\varepsilon}(\mathbf{u})\rangle = \boldsymbol{\Sigma} : \mathbf{E} \tag{22}$$

for any divergence free periodic stress field $\boldsymbol{\sigma}$ and any strain–periodic displacement field $\mathbf{u}$. Equality (22) is known as the Hill's macro-homogeneity equality.

Problem (21) exhibits two significant differences with a classical boundary problem:

- the loading consists in the integral of one field (and not in boundary or body forces);
- the boundary conditions are not local.

However, it turns out to be generally well-posed, i.e. it admits a unique solution $(\boldsymbol{\sigma}, \mathbf{u})$ up to a rigid displacement field (this has been proved for linear elasticity, perfect plasticity and linear visco-elasticity). Once $\boldsymbol{\sigma}$ and $\mathbf{u}$ are known, the missing macroscopic quantity $\mathbf{E}$ or $\boldsymbol{\Sigma}$ may be evaluated. Repeating this process for any value of $\boldsymbol{\Sigma}$ or $\mathbf{E}$ amounts to build the $\boldsymbol{\Sigma} - \mathbf{E}$ relationship, i.e. the global (macroscopic) constitutive law of the composite material. This is termed homogenization because, by definition, if masonry is replaced by the fictitious homogeneous material obeying to this macroscopic constitutive law (homogenized material), the global answer of the specimen subjected to a macroscopically homogeneous loading remains the very same. Such a result seems of little interest since, in practice, loads are hardly macroscopically homogeneous. However, it turns out to remain approximately true even for a macroscopically non-homogeneous loading provided that it does not change too much from a basic cell to the next one. This means that the global behaviour of a plane masonry structure subjected to in-plane loads is accessible without needing to represent each individual basic cell. The same structure subjected to the same loads but made of the homogenized material behaves in a similar way and is advantageously discretizable with a reasonable number of finite elements (the discretization of the original structure would be prohibitive). Furthermore, once the problem has been solved on the homogenized structure, i.e. once macroscopic stress $\boldsymbol{\Sigma}$ and strain $\mathbf{E}$ are known at each Gauss point, the corresponding microscopic stress field $\boldsymbol{\sigma}$ and displacement field $\mathbf{u}$ in the basic cell may be traced back by solving (21).

2.4. *Applicability of the homogenization theory*

As stated before, the homogenization theory applies well provided that the loading conditions are similar for adjacent basic cells. In practice, this is satsified if the size of the basic cell is very small when compared to the size of the structure; at the structural scale, two adjacent cells have almost the same position and thus undergo almost the same loading. Incidentally, this condition is fundamental for deriving the homogenization theory through asymptotic expansions with respect to the relative size of the basic cell (Bensoussan *et al.*, 1978; Duvaut, 1984; Sanchez-Palencia, 1980). However, the homogenization theory may

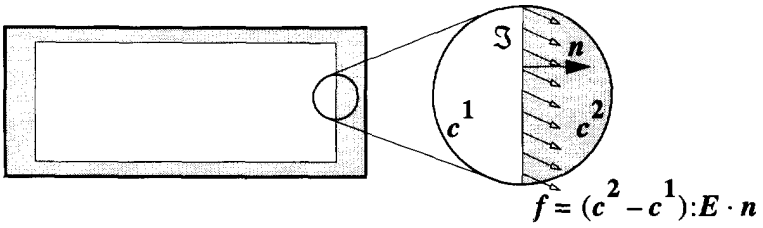

Fig. 9. Body forces concentrated at the interface of the constituents (brick and mortar).

also apply in the case of "not so small" basic cell if the macroscopic stresses induced by the structural loads vary slowly within the structure; an extreme example is the testing set-up of Fig. 5 where the induced macroscopic stresses are constant over the specimen. It is worth noting that the relative size of the cell is known *a priori* whereas the variations of the macroscopic stresses within the structure are known *a posteriori*, i.e., only once the homogenized problem has been solved. The homogenization theory also applies if the characteristics of the basic cell change slowly within the structure, i.e. if adjacent basic cells are almost identical.

Finally, concentrated loads and boundary conditions relative to the structure may cause high gradients or even singularities in the macroscopic stress field. In those regions, adjacent cells, even very small, may be found to undergo quite different loading conditions. In that case, a local study in the critical region should be performed on the original (non-homogenized) material in order to verify the validity of the global solution found on the homogenized structure.

2.5. *Homogenization in linear elasticity*

Both constituents (brick and mortar) are now assumed linear elastic and perfectly bonded. Problem (21) with strain controlled loading reads

$$\begin{aligned} \operatorname{div}\boldsymbol{\sigma} &= \mathbf{0} \text{ on } S \\ \boldsymbol{\sigma} &= \mathbf{c} : \boldsymbol{\varepsilon}(\mathbf{u}) \\ \boldsymbol{\sigma} \cdot \mathbf{n} &\text{ anti-periodic on } \partial S \\ \mathbf{u} - \mathbf{E} \cdot \mathbf{x} &\text{ periodic on } \partial S, \end{aligned} \tag{23}$$

where $\mathbf{E}$ is a given symmetric second-order tensor of $\mathscr{R}^2$ and $\mathbf{c}$ is the fourth-order tensor of elastic stiffnesses in plane stress. Writing (23) in terms of $\mathbf{u}^{\mathrm{p}} = \mathbf{u} - \mathbf{E} \cdot \mathbf{x}$, and eliminating $\boldsymbol{\sigma}$, the following system is obtained:

$$\begin{aligned} \operatorname{div}(\mathbf{c} : \boldsymbol{\varepsilon}(\mathbf{u}^{\mathrm{p}})) + \operatorname{div}(\mathbf{c} : \mathbf{E}) &= \mathbf{0} \text{ on } S \\ \mathbf{c} : (\boldsymbol{\varepsilon}(\mathbf{u}^{\mathrm{p}}) + \mathbf{E}) \cdot \mathbf{n} &\text{ anti-periodic on } \partial S \\ \mathbf{u}^{\mathrm{p}} &\text{ periodic on } \partial S. \end{aligned} \tag{24}$$

Note that the term $\mathbf{c} : (\boldsymbol{\varepsilon}(\mathbf{u}^{\mathrm{p}}) + \mathbf{E}) \cdot \mathbf{n}$ simply reduces to $\mathbf{c} : \boldsymbol{\varepsilon}(\mathbf{u}^{\mathrm{p}}) \cdot \mathbf{n}$ if the material characteristics are continuous across the boundary ∂S. The solution of (24) is then the periodic displacement field inducing a periodic stress field and equilibrating the body forces $\mathbf{f}$ induced by the uniform strain $(-\mathbf{E})$. If $\mathbf{c}$ is further assumed constant on each constituent, those body forces then reduce to concentrate forces at the interface $\mathscr{J}$ between the constituents:

$$\mathbf{f} = \operatorname{div}(\mathbf{c} : \mathbf{E}) = (\mathbf{c}^2 - \mathbf{c}^1) : \mathbf{E} \cdot \mathbf{n} \delta_{\mathscr{J}}, \tag{25}$$

where $\mathbf{n}$ is the normal oriented from material 1 to material 2 and $\delta_{\mathscr{J}}$ is the Dirac distribution on the interface $\mathscr{J}$ (Fig. 9).

Owing to the linearity of the problem, the solution $\mathbf{u}^{\mathrm{P}}$ and thus $\mathbf{u} = \mathbf{u}^{\mathrm{P}} + \mathbf{E} \cdot \mathbf{x}$ for any $\mathbf{E}$, may be found by linear recombination of the solutions corresponding to the three elementary tensors:

$$\mathbf{I}^{11} = \begin{bmatrix} 1 & 0 \\ 0 & 0 \end{bmatrix}, \quad \mathbf{I}^{22} = \begin{bmatrix} 0 & 0 \\ 0 & 1 \end{bmatrix}, \quad \mathbf{I}^{12} = \mathbf{I}^{21} = \begin{bmatrix} 0.5 & 0 \\ 0 & 0.5 \end{bmatrix} \tag{26}$$

so that, if $\mathbf{u}^{\alpha\beta}$ is the solution of (23) for $\mathbf{E} = \mathbf{I}^{\alpha\beta}$, then $\mathbf{u} = E_{\alpha\beta}\mathbf{u}^{\alpha\beta}$ is the solution for $\mathbf{E} = E_{\alpha\beta}\mathbf{I}^{\alpha\beta}$. In particular, the local strains are given by

$$\varepsilon_{\gamma\delta}(\mathbf{u}) = \varepsilon_{\gamma\delta}(E_{\alpha\beta}\mathbf{u}^{\alpha\beta}) = \varepsilon_{\gamma\delta}(\mathbf{u}^{\alpha\beta})E_{\alpha\beta} = A_{\gamma\delta\alpha\beta}E_{\alpha\beta}, \tag{27}$$

where $\mathbf{A}$ is a fourth-order tensor sometimes called the tensor of strain localization because it gives the local strains $\boldsymbol{\varepsilon}$ in terms of the average strain $\mathbf{E}$. Moreover, the average stress $\boldsymbol{\Sigma}$ is given by

$$\boldsymbol{\Sigma} = \langle \boldsymbol{\sigma} \rangle = \langle \mathbf{c} : \boldsymbol{\varepsilon}(\mathbf{u}) \rangle = \langle \mathbf{c} : \mathbf{A} : \mathbf{E} \rangle = \langle \mathbf{c} : \mathbf{A} \rangle : \mathbf{E} \tag{28}$$

so that $\mathbf{C} = \langle \mathbf{c} : \mathbf{A} \rangle$ turns out to be the macroscopic tensor of elastic stiffnesses of the equivalent two-dimensional (plane stress) material.

A dual approach would consist in solving problem (21) under stress controlled loading, i.e.

$$\begin{gathered} \operatorname{div} \boldsymbol{\sigma} = \mathbf{0} \text{ on } S \\ \boldsymbol{\varepsilon}(\mathbf{u}) = \mathbf{c}^{-1} : \boldsymbol{\sigma} \\ \boldsymbol{\sigma} \cdot \mathbf{n} \text{ anti-periodic on } \partial S \\ \mathbf{u} - \langle \mathbf{c}^{-1} : \boldsymbol{\sigma} \rangle \cdot \mathbf{x} \text{ periodic on } \partial S \\ \langle \boldsymbol{\sigma} \rangle = \boldsymbol{\Sigma}, \end{gathered} \tag{29}$$

where $\boldsymbol{\Sigma}$ is a given symmetric second-order tensor of $\mathscr{R}^2$ and $\mathbf{c}^{-1}$ is the fourth-order tensor of elastic compliances in plane stress. As this problem is linear, the solution $\boldsymbol{\sigma}$ is equal to $\Sigma_{\alpha\beta}\boldsymbol{\sigma}^{\alpha\beta}$, where $\boldsymbol{\sigma}^{\alpha\beta}$ is the elementary solution obtained for $\boldsymbol{\Sigma} = \mathbf{I}^{\alpha\beta}$. The fourth-order tensor $\mathbf{B}$, defined by

$$B_{\gamma\delta\alpha\beta} = \sigma_{\gamma\delta}^{\alpha\beta}, \tag{30}$$

is sometimes called the tensor of stress concentration because it gives the local stresses $\boldsymbol{\sigma}$ in terms of the average stress $\boldsymbol{\Sigma}$.

Finally, the average strain $\mathbf{E}$ being given by

$$\mathbf{E} = \langle \boldsymbol{\varepsilon}(\mathbf{u}) \rangle = \langle \mathbf{c}^{-1} : \boldsymbol{\sigma} \rangle = \langle \mathbf{c}^{-1} : \mathbf{B} : \boldsymbol{\Sigma} \rangle = \langle \mathbf{c}^{-1} : \mathbf{B} \rangle : \boldsymbol{\Sigma}, \tag{31}$$

$\mathbf{D} = \langle \mathbf{c} : \mathbf{B} \rangle$, turns out to be the macroscopic tensor of elastic compliances of the equivalent two-dimensional (plane stress) material. These two approaches are equivalent in the sense that they lead to the definition of the same homogeneous material ($\mathbf{D} = \mathbf{C}^{-1}$).

3. GENERALIZATION TO THREE-DIMENSIONAL PERIODIC MEDIA HAVING ONLY TWO DIRECTIONS OF PERIODICITY

The presentation of Section 2 may be easily generalized to the case of a three-dimensional composite media having three directions of periodicity. The additional direction is then treated in the same way as the other two so that the equivalent homogeneous media is also three-dimensional. In practice, this means that all indices are then varying from one

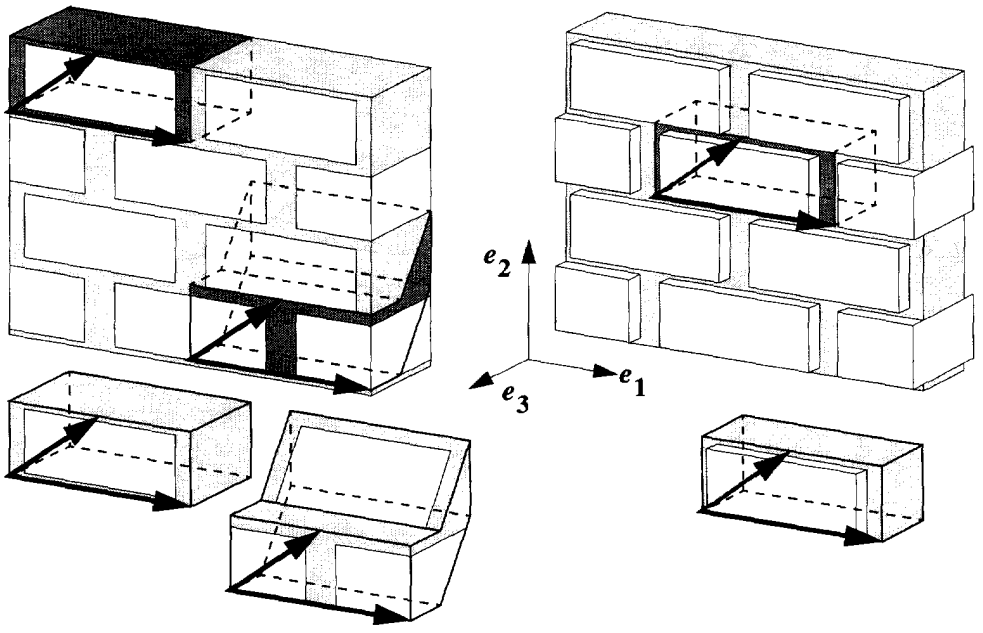

Fig. 10. Three-dimensional basic cells in the case of regular (left) or irregular (right) lateral faces.

to three (v_i, x_i, u_i E_{ij}, Σ_{ij}, etc.). Such a methodology is therefore appropriate for masonry bulks, i.e. three-dimensional periodic arrangements of brick and mortar (Fig. 11, right). Up to a certain extent, it can also be applied to masonry walls if these are considered as slices of masonry bulks, so that their homogenized in-plane characteristics coincide with those of the bulk; this is the method used in Pande *et al.* (1989) and Pietruszczak and Niu (1992). It is however an approximate method because then the lateral faces of the wall are not generally stress free, only the average of the lateral stress vector over a basic cell is zero. In reality, plane masonry is a three-dimensional media with only two directions of periodicity in its own plane. The third direction (through the thickness) should therefore be treated in a different way than the other two as is shown hereafter.

3.1. *Description of the periodic media*

Consider a portion of masonry wall in dimension three (Fig. 10). It is a three-dimensional periodic media characterised by the same two directions of periodicity as in the plane stress case. Therefore, the frame of reference ($\mathbf{v}_1$, $\mathbf{v}_2$) is still valid provided that $\mathbf{v}_1$ and $\mathbf{v}_2$ are now considered as vectors of $\mathscr{R}^3$ (having a zero component on $\mathbf{e}_3$). Basic cells are now three-dimensional; if the lateral faces of the masonry wall are plane, any of the two-dimensional basic cells S proposed in the previous section may transform into a three-dimensional basic cell V by translation along $2w\mathbf{e}_3$, where $2w$ stands for the thickness of the wall. Of course, other choices of cell are also possible (Fig. 10, left). If the lateral faces of the wall are irregular (concave joints, bricks with uneven lateral faces), the definition of the thickness is not so clear. However, this does not preclude the clear definition of a basic cell V (Fig. 10, right).

In the boundary surface ∂V of any three-dimensional cell, two different regions may be distinguished (Fig. 11, left); ∂V_i which is internal to the wall (interfaces with adjacent cells) and ∂V_e which is external (lateral faces). As in the two-dimensional case, ∂V_i may be divided into three or two pairs of identical sides corresponding to each other through a translation along $\mathbf{v}_1$, $\mathbf{v}_2$ or $\mathbf{v}_1 - \mathbf{v}_2$ (opposite sides). This is generally not true for ∂V_e; the two lateral faces are not necessarily identical and, even if it is the case, they should not be called opposite sides since they are not related by periodicity. In particular, a three-dimensional basic cell characteristic of a masonry wall should not be confused with its homologue which is characteristic of a masonry bulk having three directions of periodicity as in the above-mentioned "slice" approach. In the latter case, the frame of reference would be composed

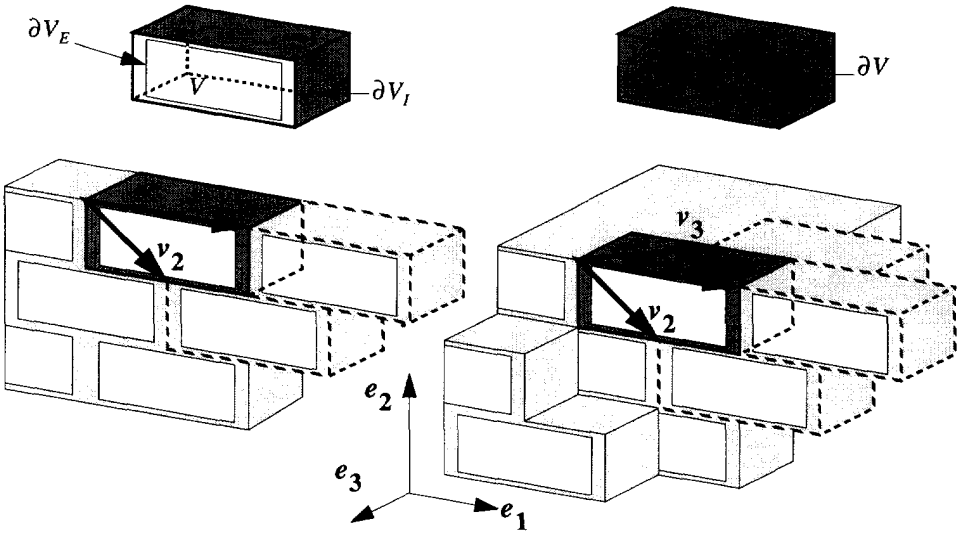

Fig. 11. Homologous basic cells defining a masonry wall (left) and a masonry bulk (right).

of three vectors and the boundary ∂V of the cell would be exclusively composed of opposite sides (Fig. 11, right).

As far as stack bond and running bond are concerned, one brick surrounded by half mortar joints still constitutes an appropriate basic cell having three planes of symmetry.

3.2. *Periodic stresses, strain–periodic displacements*

The definition of such fields need to be revised. Consider again a macroscopically homogeneous plane stress state; conditions (i) (stress compatibility) and (ii) (strain compatibility) still hold but only on the internal part ∂V_i of the boundary ∂V, the remaining part ∂V_e being stress free. Therefore, a periodic stress field is such that stress vectors are opposite on opposite sides of ∂V_i, but no similar condition is required on ∂V_e. Analogously, strain compatibility is needed only on ∂V_i, on two opposite sides of ∂V_i, the displacement fields must be equal up to a rigid displacement. For stack bond pattern, this is expressed by

$$\begin{aligned}&\forall x_2 \in [-h, h], \forall x_3 \in [-w, w], \mathbf{u}(\mathrm{l}, x_2, x_3) - \mathbf{u}(-\mathrm{l}, x_2, x_3) = \mathbf{U} + \mathbf{R} \wedge (x_2\mathbf{e}_2 + x_3\mathbf{e}_3)\\ &\forall x_1 \in [-l, l], \forall x_3 \in [-w, w], \mathbf{u}(x_1, h, x_3) - \mathbf{u}(x_1, -h, x_3) = \mathbf{V} + \mathbf{S} \wedge (x_1\mathbf{e}_1 + x_3\mathbf{e}_3),\end{aligned} \tag{32}$$

where $\mathbf{U}$ and $\mathbf{V}$ are translation vectors of $\mathscr{R}^3$, and $\mathbf{R}$ and $\mathbf{S}$ are rotation vectors of $\mathscr{R}^3$. When written for extreme values of x_1 and x_2, i.e. on edges shared by two different sides of ∂V_i, relations (32) become

$$\forall x_3 \in [-t, t], \begin{cases} x_2 = h \Rightarrow \mathbf{u}(l, h, x_3) - \mathbf{u}(-l, h, x_3) = \mathbf{U} + \mathbf{R} \wedge (h\mathbf{e}_2 + x_3\mathbf{e}_3) \\ x_2 = -h \Rightarrow \mathbf{u}(l, -h, x_3) - \mathbf{u}(-l, -h, x_3) = \mathbf{U} + \mathbf{R} \wedge (-h\mathbf{e}_2 + x_3\mathbf{e}_3) \\ x_1 = l \Rightarrow \mathbf{u}(l, h, x_3) - \mathbf{u}(l, -h, x_3) = \mathbf{V} + \mathbf{S} \wedge (l\mathbf{e}_1 + x_3\mathbf{e}_3) \\ x_1 = -l \Rightarrow \mathbf{u}(-l, h, x_3) - \mathbf{u}(-l, -h, x_3) = \mathbf{V} + \mathbf{S} \wedge (-l\mathbf{e}_1 + x_3\mathbf{e}_3) \end{cases} \tag{33}$$

Such a system is compatible if, and only if, $\mathbf{R}$ and $\mathbf{S}$ satisfy

$$2h\mathbf{R} \wedge \mathbf{e}_2 = 2l\mathbf{S} \wedge \mathbf{e}_1 \Leftrightarrow \begin{cases} R_3 = S_3 = 0 \\ 2hR_1 + 2lS_2 = 0 \end{cases}, \tag{34}$$

so that by taking $T = R_1/2l = -S_2/2h$, (23) reduces to

$$\forall x_2 \in [-h, h], \forall x_3 \in [-w, w]$$

$$\mathbf{u}(l, x_2, x_3) - \mathbf{u}(-l, x_2, x_3) = \mathbf{U} + R_2 x_3 \mathbf{e}_1 + 2lT(x_2 \mathbf{e}_3 - x_3 \mathbf{e}_2)$$

$$\forall x_1 \in [-l, l], \forall x_3 \in [-w, w]$$

$$\mathbf{u}(x_1, h, x_3) - \mathbf{u}(x_1, -h, x_3) = \mathbf{V} - S_1 x_3 \mathbf{e}_2 + 2hT(x_1 \mathbf{e}_3 - x_3 \mathbf{e}_1). \tag{35}$$

Relations (35) characterize strain–periodic displacement fields for stack bond pattern. Similar relations may be derived in the case of running pattern provided that a parallel-epipedic cell is used. In both cases, a strain–periodic displacement field may always be written in the following way:

$$\begin{aligned}
u_1(x_1, x_2, x_3) &= E_{11}x_1 + E_{12}x_2 - \chi_{11}x_1x_3 - \chi_{12}x_2x_3 + \Omega_2 x_3 + u_1^{\mathrm{P}}(x_1, x_2, x_3) \\
u_2(x_1, x_2, x_3) &= E_{21}x_1 + E_{22}x_2 - \chi_{22}x_2x_3 - \chi_{12}x_1x_3 - \Omega_1 x_3 + u_2^{\mathrm{P}}(x_1, x_2, x_3) \\
u_3(x_1, x_2, x_3) &= \chi_{11}x_1^2/2 + \chi_{22}x_2^2/2 + \chi_{12}x_1x_2 + \Omega_1 x_2 - \Omega_2 x_1 + u_3^{\mathrm{P}}(x_1, x_2, x_3),
\end{aligned} \tag{36}$$

where E_{11}, E_{12}, E_{22}, E_{21}, χ_{11}, χ_{12}, χ_{22}, Ω_1 and Ω_2 are nine constants and $\mathbf{u}^{\mathrm{P}}$ is a periodic displacement field ($\mathbf{u}^{\mathrm{P}}$ takes the same value on opposite sides of $\partial \mathrm{V}_i$). Equivalence between (35) and (36) may be easily proved by taking

$$\begin{gathered}
E_{11} = U_1/2l; \quad E_{21} = U_2/2l; \quad E_{12} = V_1/2h; \quad E_{22} = V_2/2h \\
\chi_{11} = -R_2/2l; \quad \chi_{22} = S_1/2h; \quad \chi_{12} = T \\
\Omega_1 = V_3/2h; \quad \Omega_2 = -U_3/2l.
\end{gathered} \tag{37}$$

Relations (37) show that $E_{\alpha\beta}$ still represents the mean strain tensor of the cell but in the plane $(\mathbf{e}_1, \mathbf{e}_2)$ only (second-order tensor of $\mathscr{R}^2$). As in the two-dimensional case, the anti-symmetric part of $\mathbf{E}$ may be disregarded for corresponding to a rigid rotation of the cell around $\mathbf{e}_3$. Similarly, Ω_1 and Ω_2 will not be taken into account since they also correspond to rigid rotations of the cell (around $\mathbf{e}_1$ and $\mathbf{e}_2$, respectively). The three remaining constants χ_{11}, χ_{12} and χ_{22} characterize the out-of-plane deformation of the cell (bending): for example, χ_{11} represents the mean curvature of the cell along $\mathbf{e}_1$; more generally, $\chi_{\alpha\beta}$ turns out to be the mean curvature tensor of the cell considered as a plate of normal $\mathbf{e}_3$ (χ_{21} being defined as equal to χ_{12}). Note that these constants did not appear in the two-dimensional case in Section 2 because in-plane displacements were implicitly considered. However, since the out-of-plane behaviour of masonry is not under the scope of this paper, $\chi_{\alpha\beta}$ constants will be simply zeroed from now on. Any strain–periodic displacement field $\mathbf{u}$ therefore takes the following form:

$$\left.\begin{aligned}
u_1(x_1, x_2, x_3) &= E_{11}x_1 + E_{12}x_2 + u_1^{\mathrm{P}}(x_1, x_2, x_3) \\
u_2(x_1, x_2, x_3) &= E_{21}x_1 + E_{22}x_2 + u_2^{\mathrm{P}}(x_1, x_2, x_3) \\
u_3(x_1, x_2, x_3) &= u_3^{\mathrm{P}}(x_1, x_2, x_3)
\end{aligned}\right\} \Leftrightarrow u_i(x_1, x_2, x_3) = \delta_{i\alpha}E_{\alpha\beta}\delta_{\beta j}x_j + u_i^{\mathrm{P}}(x_1, x_2, x_3), \tag{38}$$

where $\mathbf{E}$ is a symmetric second-order tensor of dimension two only, $\boldsymbol{\delta}$ is the Kronecker symbol and $\mathbf{u}^{\mathrm{P}}$ is a periodic displacement field.

As in the two-dimensional case, $E_{\alpha\beta}$ may be identified to the average of the corresponding component $\varepsilon_{\alpha\beta}$ of the microscopic strain tensor, provided that the basic cell V is suitably defined. The average of $\varepsilon_{\alpha\beta}$ is naturally given by

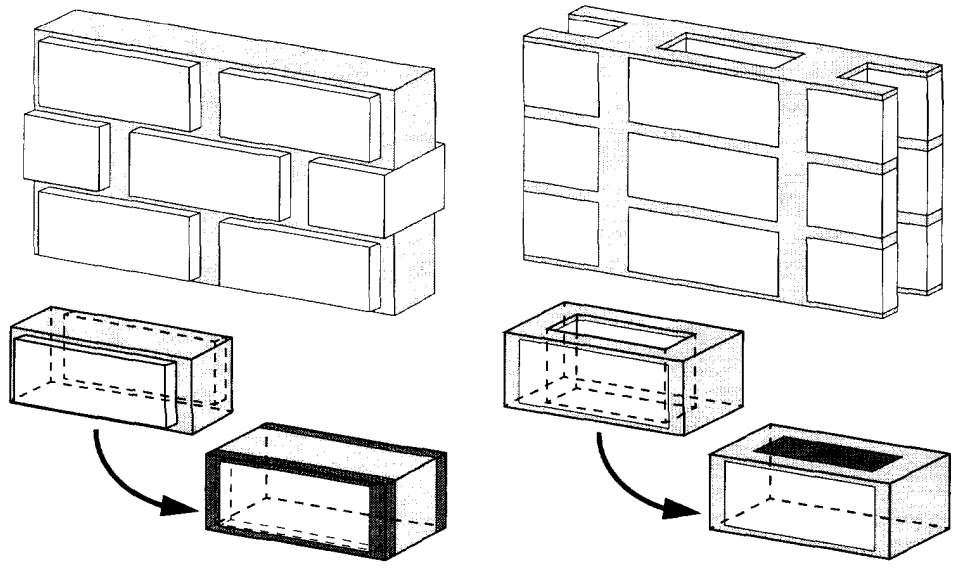

Fig. 12. Completion of basic cells having irregular lateral faces (left) or internal holes (right).

$$\langle \varepsilon_{\alpha\beta}(\mathbf{u}) \rangle = \frac{1}{|V|} \int_V \varepsilon_{\alpha\beta}(\mathbf{u}) \, \mathrm{d}v, \tag{39}$$

where $|V|$ stands for the volume of the basic cell. From (38), one gets

$$\varepsilon_{\alpha\beta}(\mathbf{u}) = E_{\alpha\beta} + (u^{\mathrm{p}}_{\alpha,\beta} + u^{\mathrm{p}}_{\beta,\alpha})/2 \tag{40}$$

so that, by introducing (40) into (39) and applying the divergence theorem, it follows that

$$\langle \varepsilon_{\alpha\beta}(\mathbf{u}) \rangle = E_{\alpha\beta} + \frac{1}{2|V|} \left(\int_{\partial V_{\mathrm{i}}} (u^{\mathrm{p}}_{\alpha} n_{\beta} + u^{\mathrm{p}}_{\beta} n_{\alpha}) \, \mathrm{d}s + \int_{\partial V_{\mathrm{e}}} (u^{\mathrm{p}}_{\alpha} n_{\beta} + u^{\mathrm{p}}_{\beta} n_{\alpha}) \, \mathrm{d}s \right), \tag{41}$$

where the boundary ∂V of V has been split into its internal and external parts. Since $\mathbf{u}^{\mathrm{p}}$ and $\mathbf{n}$ are, respectively, periodic and anti-periodic on the internal boundary ∂V_{i}, the first integral vanishes. The second integral defined on the external boundary ∂V_{e} vanishes only if the lateral faces of the basic cell are plane and perpendicular to $\mathbf{e}_3$ (i.e. if $n_1 = n_2 = 0$ on ∂V_{e}). It is always possible to choose a basic cell having such a property since the eventual irregularities of the lateral faces may be filled by a fictitious material having zero stiffness (Fig. 12, left). Of course the volume $|V|$ of the cell increases in the same proportion. Such an artifice gives the desired property

$$\langle \varepsilon_{\alpha\beta}(\mathbf{u}) \rangle = E_{\alpha\beta} \Leftrightarrow \langle \boldsymbol{\varepsilon}(\mathbf{u}) \rangle = \mathbf{E}. \tag{42}$$

Furthermore, it leads to a possible definition of the thickness of the wall as the distance separating the two artificial lateral faces. However, expression (39) needs then to be clarified since $\varepsilon_{\alpha\beta}(\mathbf{u})$ is not defined in the fictitious material. The same problem also appears in the case of internal holes (Fig. 12, right). As in the two-dimensional case, expression (39) may be transformed into a boundary integral on ∂V_{i} (∂V_{e} being chosen such that $n_1 = n_2 = 0$):

$$\langle \varepsilon_{\alpha\beta}(\mathbf{u}) \rangle = \frac{1}{2|V|} \int_{\partial V_{\mathrm{i}}} (u_{\alpha} n_{\beta} + u_{\beta} n_{\alpha}) \, \mathrm{d}s. \tag{43}$$

Expression (43) is well defined provided that ∂V_{i} does not intersect either superficial

irregularities or internal holes. Unfortunately, in dimension three, such a choice is not always possible; internal holes or superficial irregularities or both may be inevitable (Fig. 12). In that case, the definition equivalent to the one proposed at the end of Section 2.2 is then the only one available. According to definition (38), if $\mathbf{x}$ and $(\mathbf{x}+\mathbf{t})$ are two opposite points of ∂V_i (i.e. if $\mathbf{t}$ is equal to $\mathbf{v}_1$, $\mathbf{v}_2$ or $\mathbf{v}_1-\mathbf{v}_2$), one gets

$$u_i^{\mathrm{p}}(\mathbf{x}+\mathbf{t}) = u_i^{\mathrm{p}}(\mathbf{x}) \Rightarrow u_i(\mathbf{x}+\mathbf{t}) - u_i(\mathbf{x}) = \delta_{i\alpha} E_{\alpha\beta} \delta_{\beta j} t_j \Rightarrow u_\alpha(\mathbf{x}+\mathbf{t}) - u_\alpha(\mathbf{x}) = E_{\alpha\beta} t_\beta. \tag{44}$$

Writing relation (44) for another pair of opposite points related by a vector $\mathbf{t}'$ linearly independent of $\mathbf{t}$, one gets a linear system giving $\mathbf{E}$ and thus the symmetric part of $\mathbf{E}$, in terms of $\mathbf{v}_1, \mathbf{v}_2$ and of the in-plane displacements $\mathbf{u}$ at four particular points of the internal boundary of the cell. It is always possible to choose those four points in the material part of the cell, independently of the position of the cavities. As in the two-dimensional case, this definition of the average strain is restricted to strain–periodic displacement fields. Its advantage over definitions (39) and (43), is that it does not require the completion of the basic cell (in a finite element code, only the material part will be discretized) nor the explicit definition of the thickness.

For the sake of consistency with expression (39), the average of $\sigma_{\alpha\beta}$ on the cell (by definition the macroscopic stress $\Sigma_{\alpha\beta}$) should be given by

$$\langle \sigma_{\alpha\beta} \rangle = \frac{1}{|V|} \int_{V^*} \sigma_{\alpha\beta} \, \mathrm{dv}, \tag{45}$$

where V^* is the material part of the basic cell and $|V|$ its total volume (including internal holes and superficial irregularities). This definition uses the fact that $\sigma_{\alpha\beta}$ vanishes within the cavities. However, the definition of the thickness is still required to compute the total volume of the cell ($|V| = 2w \times |\mathbf{v}_1 \wedge \mathbf{v}_2|$). This drawback may be avoided by adopting plate notations: if the average stresses are defined by

$$\langle \sigma_{\alpha\beta} \rangle = \frac{1}{|S|} \int_{V^*} \sigma_{\alpha\beta} \, \mathrm{dv}, \tag{46}$$

where $|S|$ has the same meaning as before ($|S| = |\mathbf{v}_1 \wedge \mathbf{v}_2|$), the corresponding macroscopic quantities are the membrane forces $N_{\alpha\beta}$ which coincide with the linear density of forces applied to the specimen (Fig. 5). Definition (46) offers the same advantages as the last definition proposed for the average strain (the original material cell V^* may be used and no thickness need be defined) and will be therefore adopted from now on.

It must be pointed out that both average stresses $\mathbf{N} = \langle \boldsymbol{\sigma} \rangle$ and average strains $\mathbf{E} = \langle \boldsymbol{\varepsilon}(\mathbf{u}) \rangle$ are second-order tensors of dimension two only. Definitions (39) and (46) may be used to define the "missing" components (E_{i3} and N_{i3} for $i = 1$, 2 or 3). However, this is not necessary and even not always possible, for instance, expression (39) may depend on arbitrary values of the displacement field in the cavities, even if transformed through the divergence theorem into

$$\langle \varepsilon_{i3}(\mathbf{u}) \rangle = \langle \varepsilon_{i3}(\mathbf{u}^{\mathrm{p}}) \rangle = \frac{1}{2|V|} \int_{\partial V_{\mathrm{e}}} (u_i^{\mathrm{p}} n_3 + u_3^{\mathrm{p}} n_i) \, \mathrm{d}s. \tag{47}$$

On the contrary, definition (46) is always well defined but leads to zero values for N_{i3} as it will be shown in the next section.

3.3. *Homogenization*

The boundary conditions holding on the internal boundary ∂V_{i} of the basic cell have been established. Noting that the external boundary ∂V_{e} is free of stress, the problem to be solved on the basic cell is

$$\operatorname{div}\boldsymbol{\sigma} = \mathbf{0} \text{ on } V \text{ (no body forces)}$$

$$\boldsymbol{\sigma} = f(\boldsymbol{\varepsilon}(\mathbf{u})) \text{ (complete constitutive law)}$$

$$\boldsymbol{\sigma}\cdot\mathbf{n} = \mathbf{0} \text{ on } \partial V_e$$

$$\boldsymbol{\sigma} \text{ periodic on } \partial V_i \ (\boldsymbol{\sigma}\cdot\mathbf{n} \text{ anti-periodic on } \partial V_i)$$

$$\mathbf{u} - \langle\boldsymbol{\varepsilon}(\mathbf{u})\rangle\cdot\mathbf{x} \text{ (periodic on } \partial V_i)$$

$$\langle\boldsymbol{\sigma}\rangle = \mathbf{N}, \mathbf{N} \text{ given (stress controlled loading)}$$

or

$$\langle\boldsymbol{\varepsilon}(\mathbf{u})\rangle = \mathbf{E}, \mathbf{E} \text{ given (strain controlled loading)}, \tag{48}$$

where $\langle\boldsymbol{\varepsilon}(\mathbf{u})\rangle$, $\langle\boldsymbol{\sigma}\rangle$ and $\mathbf{N}$ or $\mathbf{E}$ are second-order tensors of $\mathscr{R}^2$. For the sake of conciseness, the quantity $\delta_{i\alpha}\langle\varepsilon_{\alpha\beta}(\mathbf{u})\rangle\delta_{\beta j}x_j$ has been abusively replaced by $\langle\boldsymbol{\varepsilon}(\mathbf{u})\rangle\cdot\mathbf{x}$. It is now possible to verify that the "missing" values of $\mathbf{N}$ are zero. Since $\boldsymbol{\sigma}$ is divergence free, one has

$$\sigma_{i3} = \sigma_{ij}\delta_{3j} = \sigma_{ij}x_{3,j} = (\sigma_{ij}x_3)_j - \sigma_{ij,j}x_3 = (\sigma_{ij}x_3)_j \tag{49}$$

so that definition (46) may be transformed through the divergence theorem into

$$N_{i3} = \langle\sigma_{i3}\rangle = \frac{1}{|S|}\int_{V^*}\sigma_{i3}\,\mathrm{dv} = \frac{1}{|S|}\int_{\partial V^*}\sigma_{ij}n_jx_3\,\mathrm{d}s. \tag{50}$$

This integral vanishes because the boundary ∂V^* of the material part of the cell is composed of the free stress boundaries (lateral faces and internal holes) where $\sigma_{ij}n_j = 0$ and of the internal boundary where $\sigma_{ij}n_jx_3$ is anti-periodic.

From this point, the presentation of Section 2 may be followed. The results remain formally the same, provided that the indices are suitably defined; indices related to global quantities ($\langle\boldsymbol{\sigma}\rangle$, $\langle\boldsymbol{\varepsilon}(\mathbf{u})\rangle$, $\mathbf{N}, \mathbf{E}, \mathbf{C}$) vary from one to two, whereas those related to local quantities ($\mathbf{x}, \mathbf{u}, \mathbf{u}^{\mathrm{P}}, \boldsymbol{\varepsilon}(\mathbf{u}), \boldsymbol{\sigma}, \mathbf{c}$) vary from one to three. In particular, the tensors $\mathbf{A}$ and $\mathbf{B}$ relating $\boldsymbol{\varepsilon}$ to $\mathbf{E}$ and $\boldsymbol{\sigma}$ to $\boldsymbol{\Sigma}$, respectively, have mixed indices ($A_{ij\alpha\beta}$, $B_{ij\alpha\beta}$). The macroscopic tensor of elastic stiffnesses $\mathbf{C}$ (or its inverse $\mathbf{D}$) defines the membranous behaviour of a homogeneous plate. This tensor may be compared with the one of Section 2 if divided by the thickness of the wall (if this latter is clearly identifiable).

4. NUMERICAL APPLICATION

To illustrate the method proposed in Section 3 for the determination of the in-plane elastic characteristics of masonry, the results of some numerical simulations performed within an object oriented computer code (CASTEM 2000), are now presented. Brick and mortar are assumed to be isotropic: the Young's moduli and Poisson ratios are respectively 11,000 MPa and 0.20 for the brick, 2,200 MPa and 0.25 for the mortar. The brick dimensions are 250 × 55 × 120 mm (length × height × thickness). Head and bed mortar joints are 10 mm thick. Both running bond and stack bond patterns are considered.

For comparison purposes, the predictions based on other formulations incorporating different kinds of approximations, are also given. A separation is made *a priori* between two- and three-dimensional calculations. The two-dimensional group (plane stress) is composed of:

- the method presented in Section 2. Although it was introduced just as a preliminary step towards the final method, it constitutes a reference of the two-dimensional group (its only approximation is the plane stress assumption);
- the method proposed by Maier *et al.* (1991); for running bond, the homogenization is performed in three steps but only two steps are necessary for stack bond;

- the method proposed by Pande *et al.* (1989); the homogenization is performed in two steps, head joints being introduced first;
- a variant of the "Pande" method; the two homogenization steps are inverted, bed joints being introduced first. In the case of stack bond, this method coincides with the one of Maier;
- the multi-layer approximation, also envisaged by Maier *et al.* (1991); masonry is considered as composed of alternating layers of mortar and brick (the head joints are disregarded) and is homogenized in one step.

The method proposed in Section 3 belongs to the three-dimensional group together with:

- the method proposed by Pande *et al.* (1989);
- the inverse of it;
- the multi-layer approximation.

In each group, the methods are ordered according to increasing approximation and decreasing complexity; only the two methods presented in the paper need finite element calculations, whereas any other method may be implemented analytically. The simpler the method is, the less it can distinguish between different bond patterns.

Since each pattern considered admits two orthogonal axis of symmetry, the equivalent material/plate is orthotropic. Its stiffness tensor depends on four material constants. In order to perform direct comparisons between the different methods, all results will be presented in terms of the four material coefficients E_1, E_2, ν_{12} and G_{12} (the thickness of the wall is here clearly equal to 120 mm).

4.1. *Numerical implementation*

The three elementary problems (24) for $\mathbf{E} = \mathbf{I}^{11}$, $\mathbf{I}^{22}$ and $\mathbf{I}^{12}$ (or their equivalent in the three-dimensional case) may be solved using a standard finite element method. The only difficulty is to impose periodic conditions on $\mathbf{u}^{\mathrm{P}}$. In the finite element code CASTEM 2000, this was done through Lagrange multipliers; details about this procedure are given in the Appendix.

The periodic conditions may be reduced to ordinary Dirichlet conditions if the pattern is rectangular ($\mathbf{v}_1 \perp \mathbf{v}_2$) and if the basic cell admits two orthogonal axis/planes of symmetry (stack bond and English bond, for example). In that case, each elementary problem may be solved on a quarter cell with ordinary boundary conditions resulting from the combination of periodicity and symmetry ($\mathbf{E} = \mathbf{I}^{11}$ or $\mathbf{I}^{22}$) or periodicity and anti-symmetry ($\mathbf{E} = \mathbf{I}^{12}$) [Fig. 13(a)]. In the other cases, non-local boundary conditions subsist even if the reduction to a quarter cell may remain possible; the case of stack bond pattern is shown in Fig. 13(b). Nevertheless, hexagonal patterns may often be considered as rectangular ones by choosing cells greater than necessary; this holds true for stack bond [Fig. 13(c)], Dutch bond and Flemish bond.

However, the periodicity conditions remain inevitable as soon as the periodic pattern does not admit a cell with two orthogonal axis/planes of symmetry and an orthogonal frame of reference (1/3 running bond, for example). They are also always necessary when a non-linear behaviour is considered. Then the superimposition principle does not apply any more so that it is not sufficient to study separately the effect of each macroscopic strain component. In the presence of cavities, it will be advisable to choose the basic cell so as to minimize the number of nodes related by periodicity; for example, the right cell of Fig. 8 will be more economic than the left one.

4.2. *Homogenization under the plane stress assumption*

The results are summarized in Table 1. Only three significant digits are displayed for the values obtained through finite element computations (first two rows of results), whereas four are displayed in the case of analytical calculations. From the comparison of the two first rows, it turns out that the bond pattern (stack bond or running bond) has very little influence (less than 1% difference). In both cases, there is in fact a marked anisotropy

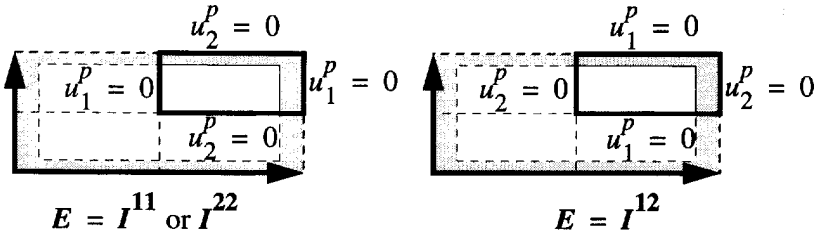

(a) Stack bond pattern

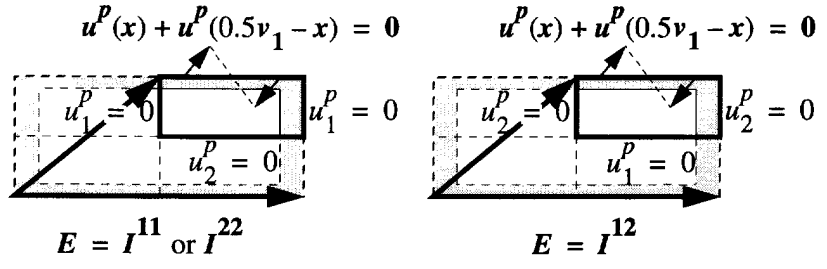

(b) Running bond pattern

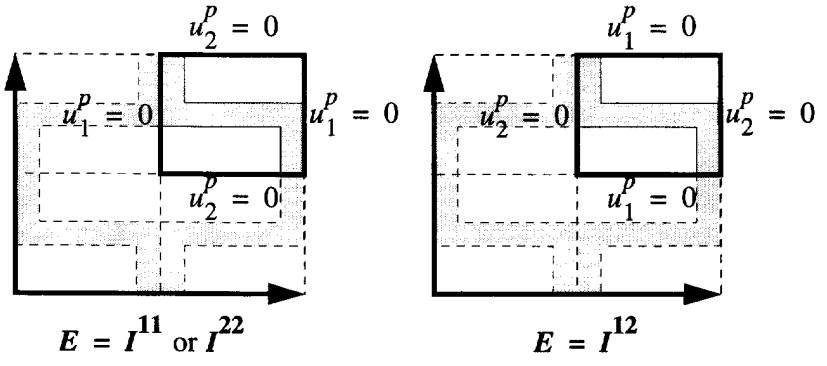

(c) Running bond pattern (double cell)

Fig. 13. Periodic boundary conditions holding on a quarter cell.

Table 1. Elastic constants of the homogenized material; two-dimensional methods

Two-dimensional homogenization (plane stress)	E_1 (MPa)	E_2 (MPa)	ν_{12}	G_{12} (MPa)
Stack bond	8530	6790	0.196	2580
Running bond	8620	6770	0.200	2620
Running bond in three steps (Maier *et al.*, 1991)	9208	6680	0.2045	2569
Running or stack bond in two steps, head joints first (Pande *et al.*, 1989)	8464	6831	0.2182	2569
Running or stack bond in 2 steps, bed joints first ("Pande inverted" or "Maier" for stack bond)	8587	6768	0.1948	2569
Multi-layer (Maier *et al.*, 1991)	9646	6950	0.2077	2782

characterized not only by the difference between the Young's moduli E_1 and E_2 (around 25%), but also by the low value of the shear modulus G_{12}.

When compared with the finite element approach, any one of the four approximated methods gives acceptable results but, surprisingly enough, the more elaborated one (approach in three steps) is not the more accurate; for running bond, the best results are obtained with the method in two steps (bed joints first). The largest error is found with the

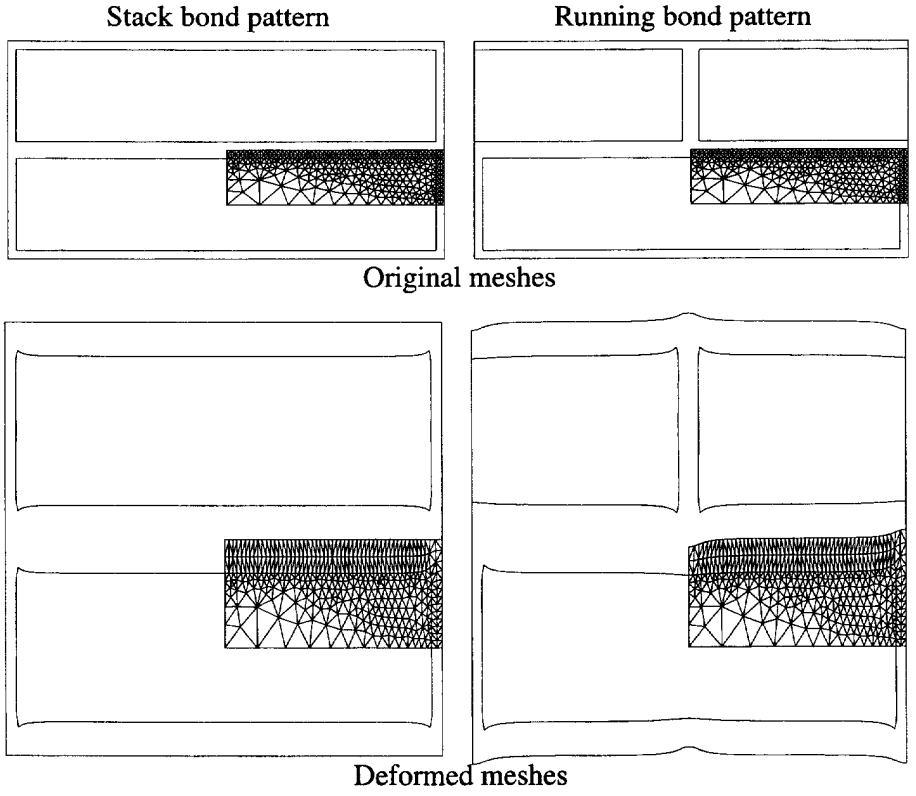

Fig. 14. Original and deformed mesh for stack bond and running bond under a vertical extension $\mathbf{E} = \mathbf{I}^{22}$ (plane stress finite element method).

simplest approach (multi-layer); the Young's and shear moduli are then systematically overestimated (up to 13%), which is logical since the head joints are assumed to be filled with the (stiffer) brick material. For the other three methods, the error is less than 7%. However, these conclusions should not be generalised since the relative accuracy of the different methods may depend on the set of data (bond pattern and material properties). As announced in the Introduction, the order of the successive steps does influence the results (rows 4 and 5).

Some comparison may also be performed between the local fields developing in the basic cell for a given macroscopic loading. For instance, the influence of the bond pattern on the displacement field is illustrated in Fig. 14 where the deformed configuration corresponds to the solution of the elementary problem for $\mathbf{E} = \mathbf{I}^{22}$, note the influence of the boundary conditions, the only thing which changes between the two calculations. Similarly, the component σ_{11} of the stress field for $\mathbf{\Sigma} = -30\mathbf{I}^{22}$ (i.e. for a vertical compression of 30 MPa) is displayed in Fig. 15; note the over-stressing of the brick induced by the head joints in the running bond pattern. In the same figure the results obtained with the analytical methods (on smaller cells below) are also shown and their approximate character is substantiated. The stress field is piece-wise constant over the basic cell, and the stress continuity is often transgressed at the interface between constant zones. Moreover, some discrepancy may be observed especially in the head joint where the value of the component σ_{11} varies from -2.5 to 1.1 MPa according to the method used. In the brick and the bed joints, however, all methods inclusive the numerical one, are in fair agreement. Remember that the above results are approximate since they were all obtained under the plane stress assumption.

4.3. *Three-dimensional homogenization*

The results summarized in Table 2 suggest the same comments as in the previous section; marked anisotropy, scarce influence of the bond pattern, systematic overestimation

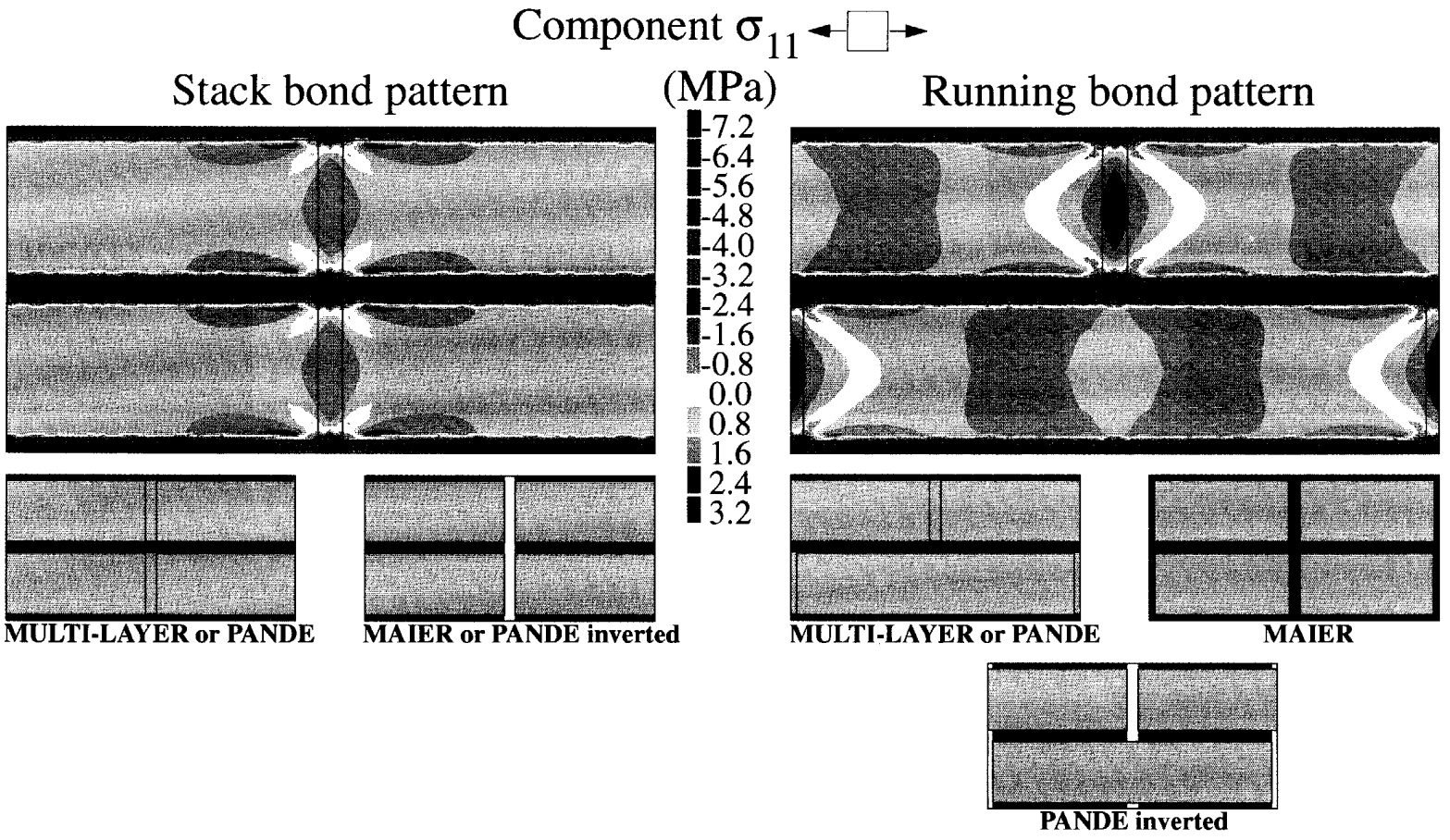

Fig. 15. Component σ_{11} of the stress field for stack bond and running bond under a uniaxial vertical compression $\Sigma_{22} = -30$ MPa (plane stress methods).

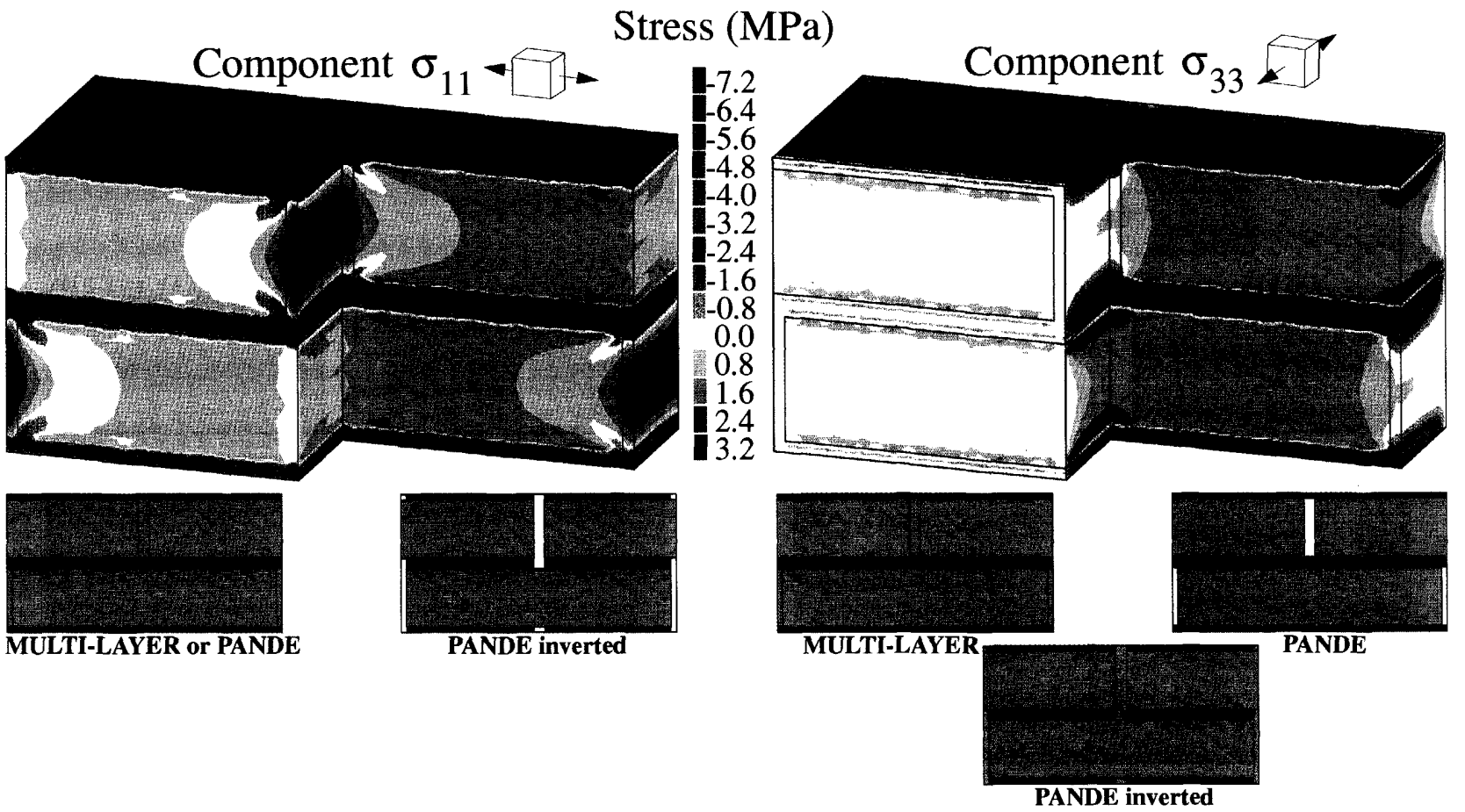

Fig. 16. Components σ_{11} (left) and σ_{33} (right) of the stress field for running bond under a uniaxial vertical compression $\Sigma_{22} = -30$ MPa (three-dimensional methods).

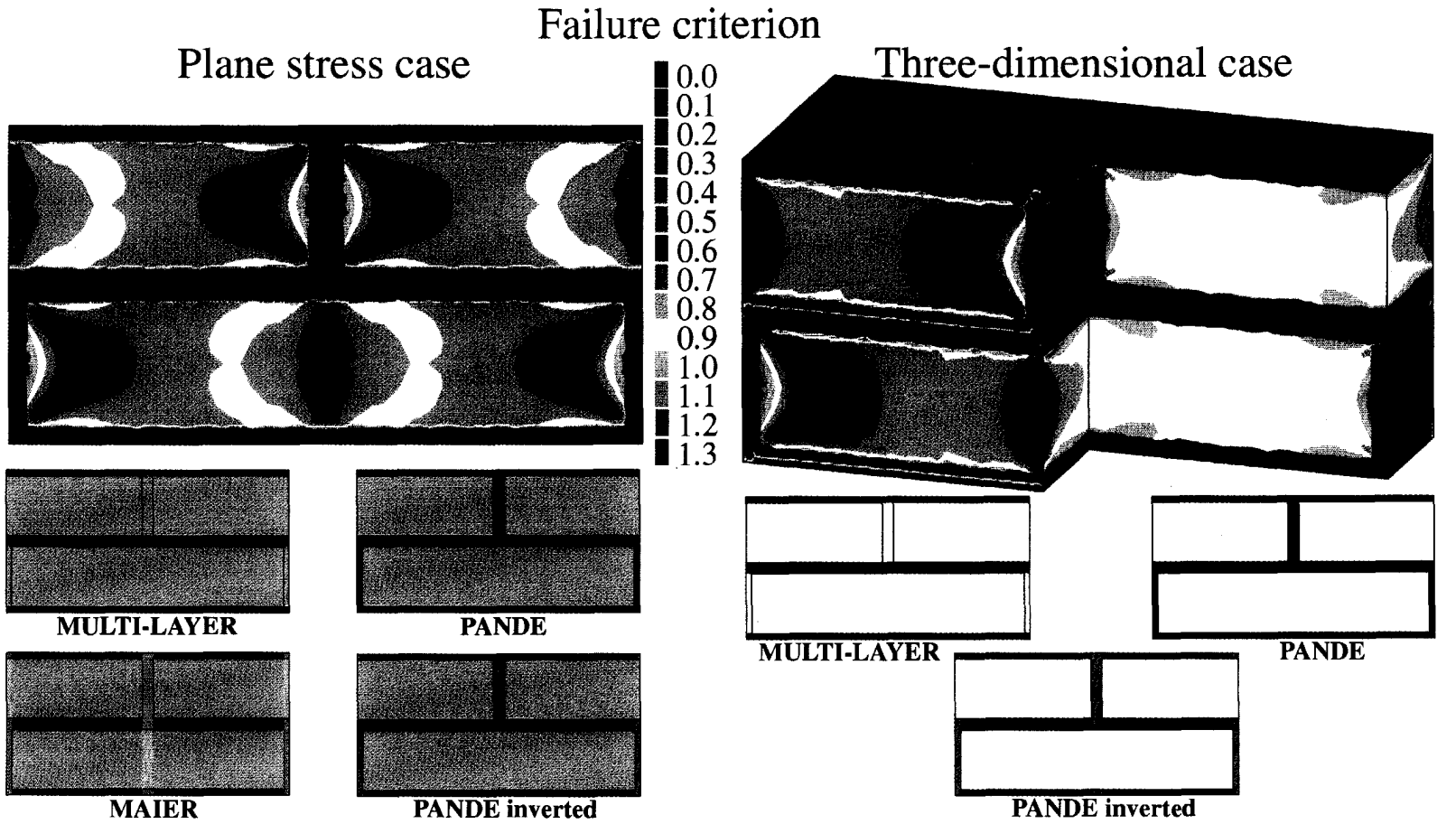

Fig. 17. Isovalues of the Mohr–Coulomb failure criterion for running bond under a uniaxial vertical compression $\Sigma_{22} = -30$ MPa; plane stress (left) and three-dimensional (right) methods.

Table 2. Elastic constants of the homogenized material; three-dimensional methods

Three dimensional homogenization	E_1 (MPa)	E_2 (MPa)	ν_{12}	G_{12} (MPa)
Stack bond	8600	7000	0.200	2580
Running bond	8680	6980	0.204	2620
Running or stack bond in two steps, head joints first (Pande *et al.*, 1989)	8566	7066	0.1974	2569
Running or stack bond in two steps, bed joints first ("Pande inverted")	8676	7006	0.1995	2569
Multi-layer	9647	7198	0.2098	2782

by the multi-layer approach, influence of the order of the successive steps. The components σ_{11} and σ_{33} of the local stress field for $\mathbf{\Sigma} = -30\mathbf{I}^{22}$ are represented in Fig. 16, only in the case of running bond. For the finite element approach, the wall is partially cut so as to see what occurs inside. Indeed, both components do vary through the thickness of the wall. This is particularly true for σ_{33} which starts from zero on the lateral faces and quickly reaches the same order of magnitude as σ_{11} inwards. For the approximate methods, only a section of the wall (slice) needs to be displayed because the stresses are constant throughout the thickness. These stresses are representative of a very thick wall (the components σ_{i3} are zero only in average) and must therefore be compared with the mid-section of the true three-dimensional wall. The stresses developing inside the wall are indeed well captured by any of the approximated methods, except in the head joints where divergences are again observed.

4.4. *Synthesis of the results*

The two groups are now put together. For a given bond pattern and a given method, the two-dimensional variant always gives lower values than the three -dimensional one. This could have been foreseen; the plane stress assumption amounts to neglect the thickness of the wall and therefore to weaken it. Conversely, the approximate three-dimensional methods suppose the wall very thick and therefore strengthen it. Only the three-dimensional finite element approach takes into account the actual thickness. Even so, the differences between the two- and three-dimensional results remain below 4%, i.e. comparable to the error related to the approximate character of the methods.

The in-plane components of the two- and three-dimensional local stress fields (σ_{11}, σ_{22} and σ_{12}) are quite similar (see, for example, σ_{11} in Figs 15 and 16). However, the out-of-plane components σ_{13}, σ_{23} and σ_{33}, which are by definition zero in the two-dimensional approach, may differ strongly (see σ_{33} in Fig. 16). Such a fact seems to have little influence on the in-plane elastic characteristics (the homogenized constants are only slightly modified), but might be crucial in the non-linear range (failure). A simple check will now provide support for this theory.

Assume the resistance of both constituents to be ruled by a Mohr–Coulomb criterion, the tension and compression limits, f_t and f_c, being, respectively, 5.2 MPa and 52 MPa for the brick, 0.5 MPa and 14 MPa for the mortar. A rough insight into the failure of masonry under vertical compression may be obtained by plotting the isovalues of the failure criterion for the elastic stress field, i.e. the quantity $(\sigma_I/f_t - \sigma_{III}/f_c)$, where $\sigma_I \geqslant \sigma_{II} \geqslant \sigma_{III}$ are the principal stresses of $\boldsymbol{\sigma}$. The predictions based on all the methods are presented in Fig. 17 (running bond masonry under a vertical compression of 30 MPa). In the two-dimensional finite element case, head and bed joints are far beyond failure, whereas the criterion is not reached in the brick yet. In the three-dimensional case, the same situation is encountered but only in a thin layer near the lateral faces. In the inner part of the wall, things are somehow inverted unless in the head joint; the bed joint is far from failure whereas the brick is about to fail. This is obviously due to the component σ_{33} of the three-dimensional stress field which is negative (compression) in the bed joint and positive (tension) in the brick as it may be seen in Fig. 16. This disagreement between the two- and three-dimensional analyses is reproduced by all the approximate methods, especially in the bed joint and in

the brick. It is therefore most probable that the conclusions drawn in the elastic range are erroneous in the non-linear range, in particular:

- the plane stress assumption may lead to erroneous results quantitatively (underestimate of the ultimate load) as well as qualitatively (wrong failure mechanism);
- the bond pattern may strongly influence the failure mechanism and consequently the failure load. For instance, under vertical compression, cracks may develop easily in the aligned head joints of stack bond masonry but need to pass through or around the brick in running bond masonry.

Of course, those conjectures need to be confirmed by performing effectively non-linear computations, for example, with damage or plasticity constitutive laws. The elementary problem (21) or (48) is then solved for a given macroscopic loading history. However, since the superposition principle does not apply anymore, the complete determination of the homogenized constitutive law requires an infinite number of computations (one for each possible loading history). Nevertheless, simplified models may be built on the basis of crude approximations of the local stress fields determined from selected loading histories. The reader is referred to Suquet (1987) who provided a comprehensive study of the homogenization theory for elastic–perfectly plastic materials.

5. CONCLUSION

The homogenization theory for periodic media has been applied in a rigorous way for deriving the in-plane elastic characteristics of masonry. In particular, the real geometry (bond pattern and finite thickness of the wall) has been taken into account. The results obtained constitute a reference basis for evaluating the relevance of some assumptions/approximations commonly used in the literature. As a matter of fact, the numerical applications performed showed that varying the bond pattern, neglecting the head joints or assuming plane stress states, result in quite reasonable estimates of the global elastic behaviour of masonry. However, a careful examination of the elastic stresses that develop in the different constitutive materials (brick and mortar) anticipate that the situation might be quite different in the non-linear range (damage or plasticity). In particular, the plane stress assumption is controversial since it is in disagreement with the exact three-dimensional analysis.

REFERENCES

Bensoussan, A., Lions, J. -L. and Papanicolaou, G. (1978). *Asymptotic Analysis for Periodic Structures*. North-Holland, Amsterdam.

Dhanasekar, M., Page, A. W. and Kleeman, P. W. (1982). The elastic properties of brick masonry. *Int. J. Masonry Constr.* **2**(4), 155–160.

Duvaut, G. (1984). Homogénéisation et matériaux composites. In *Trends and Applications of Pure Mathematics to Mechanics* (Edited by P. G. Ciarlet and M. Roseau), Lecture Notes in Physics, Vol. **195**, pp. 35–62. Springer-Verlag, Berlin.

Geymonat, G., Krasucki, F. and Marigo, J. -J. (1987). Sur la commutativité des passages à la limite en théorie asymptotique des poutres composites. *C. R. Acad. Sci. Paris*, **305**, Série II, 225–228.

Maier, G., Nappi, A. and Papa, E. (1991). Damage models for masonry as a composite material: a numerical and experimental analysis. In *Constitutive Laws for Engineering Materials* (Edited by C. S. Desai, E. Krempl, G. Frantziskonis and H. Saadatmanesh), pp. 427–432. ASME, New York.

Pande, G. N., Liang, J. X. and Middleton, J. (1989). Equivalent elastic moduli for brick masonry. *Computers Geotech.* **8**(5), 243–265.

Pietruszczak, S. and Niu, X. (1992). A mathematical description of macroscopic behaviour of brick masonry. *Int. J. Solids Structures* **29**(5), 531–546.

Sanchez-Palencia E. (1980). Non homogeneous media and vibration theory. Lecture Notes in Physics, Vol. **127**, Springer-Verlag, Berlin.

Suquet, P. -M. (1987). Elements of homogenization for inelastic solid mechanics. In *Homogenization Techniques for Composite Media* (Edited by E. Sanchez-Palencia and A. Zaoui), pp. 193–279. Springer-Verlag, Berlin.

APPENDIX

Imposing periodic conditions on the displacements through Lagrange multipliers

Once it has been discretized by finite elements, any elastic problem defined on a domain V takes the following form:

$$\mathbf{KU} = \mathbf{F}, \tag{A1}$$

where $\mathbf{U}$ is the vector containing all the degrees-of-freedom (displacements), $\mathbf{K}$ is the stiffness matrix and $\mathbf{F}$ the vector of the nodal forces (volumetric and/or boundary loads). In order to become definite, the linear system (51) must be supplemented with Dirichlet conditions, at least for controlling the rigid body motions of the domain V. These conditions may be written under the general form

$$\mathbf{AU}^0 = \mathbf{B}, \tag{A2}$$

where $\mathbf{A}$ is a rectangular matrix, $\mathbf{U}^0$ is the degree-of-freedom subjected to Dirichlet conditions and $\mathbf{B}$ is a given second member. A Dirichlet condition may consist in assigning a fixed value to a displacement at a given point. It may also consist in imposing relations between the displacements at different points. This is precisely the case of the periodic conditions, where the displacements of any opposite points of the boundary of the cell must be equal.

In many finite element codes, the problem (A1)+(A2) is solved by modifying the terms of $\mathbf{K}$ and $\mathbf{F}$ in order to take into account (A2) (for example, by elimination or penalisation). However, such modifications may become impracticable when the Dirichlet conditions are complex (relations involving several degrees-of-freedom).

In the finite element code CASTEM 2000, the Dirichlet conditions (52) are imposed through Lagrange multipliers. Instead of modifying the terms of $\mathbf{K}$ and $\mathbf{F}$, the set of unknowns $\mathbf{U}$ is augmented by two vectors $\mathbf{\Lambda}^1$ and $\mathbf{\Lambda}^2$, having the same dimension as $\mathbf{B}$, and the elastic functional of the original problem (A1), i.e.

$$W = \tfrac{1}{2}\mathbf{U}^{\mathrm{T}}\mathbf{KU} - \mathbf{U}^{\mathrm{T}}\mathbf{F} \tag{A3}$$

is modified into

$$W^* = W + \mathbf{\Lambda}_1^{\mathrm{T}}(\mathbf{AU}-\mathbf{B}) + \mathbf{\Lambda}_2^{\mathrm{T}}(\mathbf{AU}-\mathbf{B}) + \tfrac{1}{2}(\mathbf{\Lambda}_1-\mathbf{\Lambda}_2)^{\mathrm{T}}(\mathbf{\Lambda}_1-\mathbf{\Lambda}_2). \tag{A4}$$

The minimization of W^* leads to a well-conditioned symmetric linear system provided that $\mathbf{K}$ is also a well-conditioned symmetric matrix. Its solution is composed of the vector $\mathbf{U}$ verifying (A1)+(A2), and of two vectors $\mathbf{\Lambda}_1$ and $\mathbf{\Lambda}_2$ which are obviously equal and correspond to the reaction forces associated with the Dirichlet boundary conditions (52).

Although this method may appear quite heavy (two more unknowns are needed for each Dirichlet condition), its general character is a strong advantage when implementing the homogenization method described in this paper.